國立臺灣大學電機資訊學院電機工程學系

博士論文

Department of Electrical Engineering

College of Electrical Engineering and Computer Science

National Taiwan University

Doctoral Dissertation

電腦輔助之帕金森步態辨識與量化-使用單一影像序列

Computer Vision-Aided Quantification and Recognition of Parkinsonian Gait - Using Monocular Image Sequences

陳士維

Shih-Wei Chen

指導教授： 陳適卿 教授

賴金鑫 教授

郭德盛 教授

Advisors: Shih-Ching Chen, Prof.

Jin-Shin Lai, Prof.

Te-Son Kuo, Prof.

中華民國 101 年 3 月

March 2012

口試委員會審定書

國立臺灣大學博士學位論文

口試委員會審定書

電腦視覺輔助之帕金森步態辨識與量化-使用單一影像序列

Computer vision aided quantification and recognition of parkinsonian gait - using monocular imaging sequence

本論文係陳士維君在國立臺灣大學電機工程學系完成之博士學位論文，於民國一百零一年一月二十八日承下列考試委員審查通過及口試及格，特此證明。

口試委員：陳延卿 賴金鑫 郭斯彥（簽名）
（指導教授）

康立穎

陸哲駒

陳友倫

系主任 顏炳郎（簽名）

誌謝

本論文得以完成，首先得感謝郭德盛教授在我博士生涯中的啟迪與大大小小的幫助。而陳適卿教授與賴金鑫教授在學術研究方面對我的耐心指導以及提點，實惠我良多。恩師們的提攜之情，實難在寥寥數筆間盡述完畢，在此謹獻上最誠懇的敬意與謝意。陳右穎教授在研究過程中提供的絕大助力，讓我無時感念在心。此外，感謝趙福衫教授、陳友倫教授以及陸哲駒教授給予的指正與建議，本論文才得以完整面貌面世。

特別要感謝陳俊凡博士，在我博士生涯中屢屢為我指點迷津，增長我的學識，提供及協助我取得許多寶貴的資源。林穎聰學友、侯政宏學弟、郭易軒學弟等人亦功不可沒。由於有上述諸位的鼎力相助，我方能取得學位。

感謝國智與致良這兩位我最好的朋友，你們的適時鼓勵與支持，是讓我度過重重難關的最大助力之一。

最後，謹將此論文獻給我敬愛的父母親，我親愛的女友以及我友愛的兩位妹妹。因為擁有你們對我的愛與陪伴，我才能夠走過這段辛苦的歷程。

中文摘要

帕金森氏症是一種神經退化疾病，起因於中腦處黑質紋狀體中的多巴胺神經細胞的逐漸退化或死亡。步態的失序為帕金森氏症為主要的臨床表徵之一，會出現於輕度的帕金森患者身上。故而帕金森氏症患者的步態分析成為臨床醫師辨別患者與進行治療的重要依據。現有的步態量測技術如 Vicon 動作分析系統是一個高精度與信效度的步態量測工具，然而 Vicon 系統不易架設於一般診所或住家中，使得帕金森氏症步態分析受到極大的限制。為解決此一問題，本論文提出兩個利用電腦輔助的單一影像序列處理方法來協助分析輕度帕金森步態。

第一研究階段是用核心主成份分析法來量化與辨識穩定行走期的輕度帕金森步態。實驗環境需要布置一與患者有強烈對比色差的背景及一 6 公尺長的步道；實驗設備為一手持式數位單眼攝影機，從受試者側面拍攝步態啟動時與穩定行走狀態時的步行表現。結果顯示核心主成份分析法在辨別健康受試者、輕度帕金森病患在接受左多巴治療前、以及接受左多巴治療後的步態表現時，使用核心主成份分析法可以獲得高達 80.51%的敏感度；使用核心主成份分析法也可以輕易取得量化的步態參數。而步態在頻譜上的能量分佈顯示接受左多巴治療前的輕度帕金森患者的步態能量頻譜主頻帶顯著低於健康受試者及接受左多巴治療後的輕度帕金森患者兩個族群的的步態能量頻譜主頻帶。量化的時域步態參數和由輕度帕金森氏症統一評分量表之三擷取出的五種動作指標分數的關連性則顯示，量化的步態參數也可以反映出輕度帕金森患者的上肢動作障礙嚴重程度。

步態啟動表現以及步態對稱性也是用來辨別與治療輕度帕金森患者的重要依據。由於第一研究階段使用的方法仍有極大的空間限制，無法在某些僅能提供有限空間的診所使用。因而在第二研究階段，中心追蹤演算法被用來量化健康受試者、輕度帕金森病患在接受左多巴治療前、以及接受左多巴治療後的步態啟動表現以及步態對稱性。希望藉由量化的步態啟動表現以及步態對稱性，能快速且準確的辨識出輕度帕金森病

患，以及追蹤輕度帕金森病患的疾病進程。第二研究階段的實驗需要在受試者的腓骨頭與腳踝側面各黏貼一與背景有強烈對比的彩色標誌；實驗設備仍為一手持式數位單眼攝影機，用以從受試者側面拍攝步態啟動時與穩定行走狀態時的步行表現。結果顯示，中心追蹤演算法可以協助研究人員量化受試者的步態啟動與穩定行走狀態期間的步態表現與對稱性；量化數據則指出輕度帕金森患者在步態啟動與穩定行走期間的步態對稱性均顯著劣於健康受試者。此發現顯示只要使用步態啟動期間的步態對稱性即可辨識出輕度帕金森氏患者；此外，量化的步態表現數據亦可用於協助臨床人員區分輕度帕金森患者的病情以及了解患者接受藥物或復健治療後的改善情形。在實驗設置及演算法經過調整後，基於中心追蹤演算法的步態分析方法也可用於協助臨床醫師量化與辨識如腦部損傷或脊髓損傷等其他神經肌肉病患的步態。

關鍵字：電腦輔助、單一序列影像、帕金森氏症、步態分析、核心主成份分析法、統一帕金森氏症評分量表之三、中心追蹤演算法、步態啟動、步態對稱性。

Abstract

Parkinson's disease (PD) is a neurodegenerative disease of the central nervous system resulting from the death of dopamine-controlling cells in the substantia nigra within the mid-brain. Gait disorders present as cardinal motor symptoms and may be observed in early stages of the disease; therefore, the assessment of gait performance during walking has become an important reference for identification of people with PD and medical treatments. However, current available techniques for gait analysis, such as the Vicon motion analysis system with validity, reliability, and high precision, are not easily accessible in clinics or even at home for clinicians and researchers. Herein, we present two computer-aided gait analysis methods utilizing the monocular image sequences of walking to track and analyze the parkinsonian gait pattern.

The first method uses kernel-based principal component analysis (KPCA) is developed to assist the recognition and quantification of mild parkinsonian gait during the steady-state walking. It requires a digital camcorder to capture the lateral view of each subject's walking silhouette and a decorated corridor setup. The KPCA is verified to have higher sensitivity, 80.51% in this study, than the traditional image area and principal component analysis (PCA) approaches for classifying non-PD subjects and patients with mild PD in the "Drug-Off/On" states. Quantitative gait parameters are obtained and the power spectrums of the patient' gaits are analyzed. It is found that the patients with mild PD in the Drug-Off state show a lower main power spectral frequency than those of the non-PD subjects and patients with mild PD in the Drug-On state. In addition, the correlations between five subscores based on the unified Parkinson's disease rating scale (UPDRS) part III motor scores and the extracted kinematic gait parameters are discussed. Results show the feasibility of using gait performance to evaluate the motor function of upper extremity of

patients with mild PD.

The disordered gait initiation and walking asymmetry are instructors of postural instability and represent the major symptoms in the early stage of this disease except the affected gait performance. To provide the recognition and quantification of mild parkinsonian gait in clinics with too small space to deploy a corridor. The second method using the centroid tracking algorithm (CTA) is developed to quantify each subject's gait parameters and the associated symmetry indexes during the gait initiation and steady-state walking periods. This method requires only a digital camcorder to capture the lateral view of each subject's walking and two identifiers respectively secured at two palpable anatomic landmarks, the fibula head and lateral malleolus. The second method therefore becomes easier to install and use in clinics than the first one.

Results in this study indicate that the method using the CTA can help clinicians and researchers quantify the gait performance and associated symmetry indexes among age-matched non-PD subjects and patients with mild PD in different states. Quantitative analysis reveals that the age-matched non-PD subjects presented superior gait performance and associated symmetry indexes to the patients with mild PD in the different states. The findings in this study suggest that the recognition of patients with mild PD can be easily attained using only the gait symmetry indexes during the gait initiation period, indicating the cost and effort for diagnosis of PD in the early stages can be reduced largely. Besides, the quantification of gait performance may assist the clinicians to rate the severity of and monitor the progression of PD, and evaluate the therapeutic effect brought about by drug management or rehabilitation programs. In addition to performing gait analysis for patients with mild PD, we believe that the proposed portable system has the potential to help clinicians and researchers assess the gait performance of patients with other neuromuscular

issues, such as traumatic brain injury and spinal cord injury.

Keywords: computer-aided, monocular image sequence, Parkinson's disease, gait analysis, kernel-based principal component analysis, unified Parkinson's disease rating scale part III, centroid tracking algorithm, gait initiation, gait symmetry.

Contents

Figures

Tables

Chapter 1 Introduction

1.1 Parkinson's disease

1.1.1 Pathophysiology

Parkinson's disease (PD) was first and foremost described as a disease that would bear his/her name. A British apothecary named James Parkinson published a scientific article: An Essay on the Shaking Palsy [1], to unveil the motor symptoms and different stages of the morbid progress in 1817. However, the term "shaking palsy" has been vaguely employed by medical writers in general. The term "Parkinson's disease" was coined in 1870s by a French neurologist, Jean-Martin Charcot, who brought Parkinson's disease to international attention. At present, PD is the second most common neurodegenerative disorder after Alzheimer's disease and is expected to impose an increasing social and economic burden on societies as people age [2]. Due to a selective and progressive loss of dopaminergic cells, the substantia nigra pars compacta within the ventral tegmental area (VTA) of the midbrain supplies the corpus striatum (located in the basal ganglia, responsible for balance, control of movements, and walking), , and frontal cortex (responsible for thought, memory or behavior) with depleted dopamine, a catecholamine neurotransmitter plays an important role in the regulation of reward and movement. As results, the acetylcholine output elevates and therefore the equilibrium between dopamine and acetylcholine disrupts to lead motor disorder, especially fine tuning, and a breakdown in cognitive control [3].

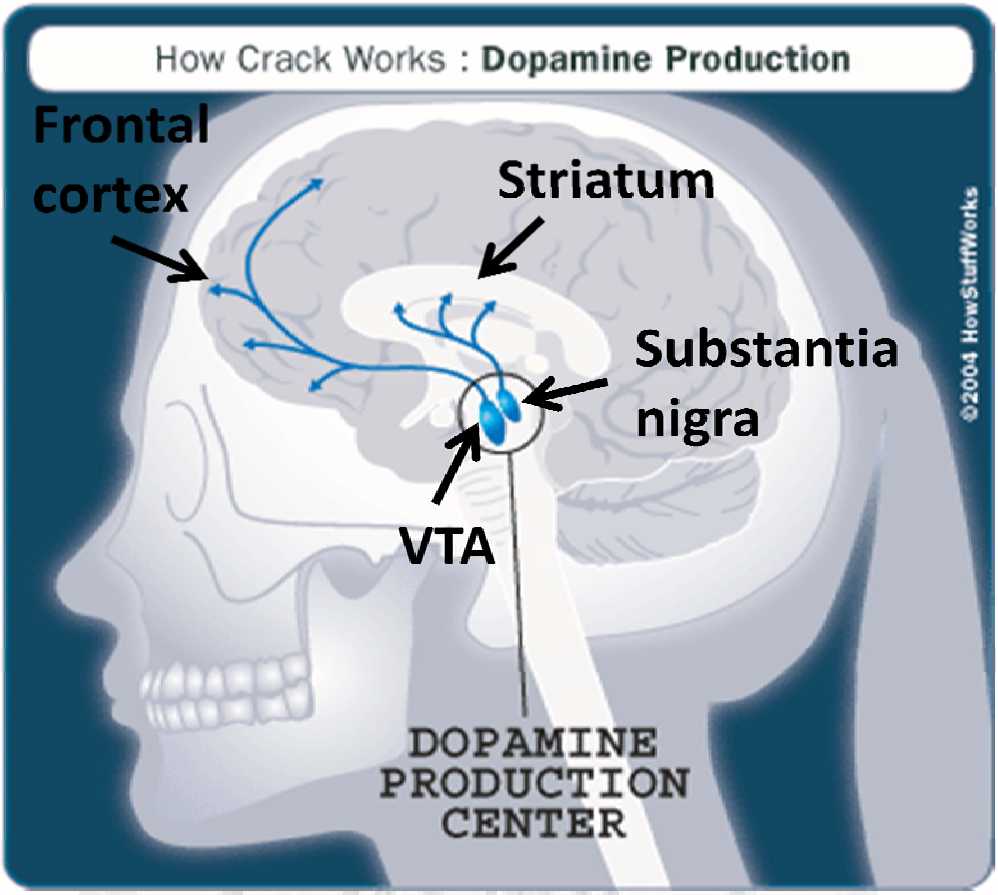

Figure 1.1 Dopamine is manufactured in nerve cell bodies located within the ventral tegmental area (VTA) and is released in the striatum and the frontal cortex (modified from [4]). People with PD may suffer from the loss of dopamine.

1.1.2 Clinical signs of Parkinson's disease

The diagnosis of PD is based on the presence of the classic clinical signs: resting tremor, rigidity, postural instability, and bradykinesia etc. [5, 6].

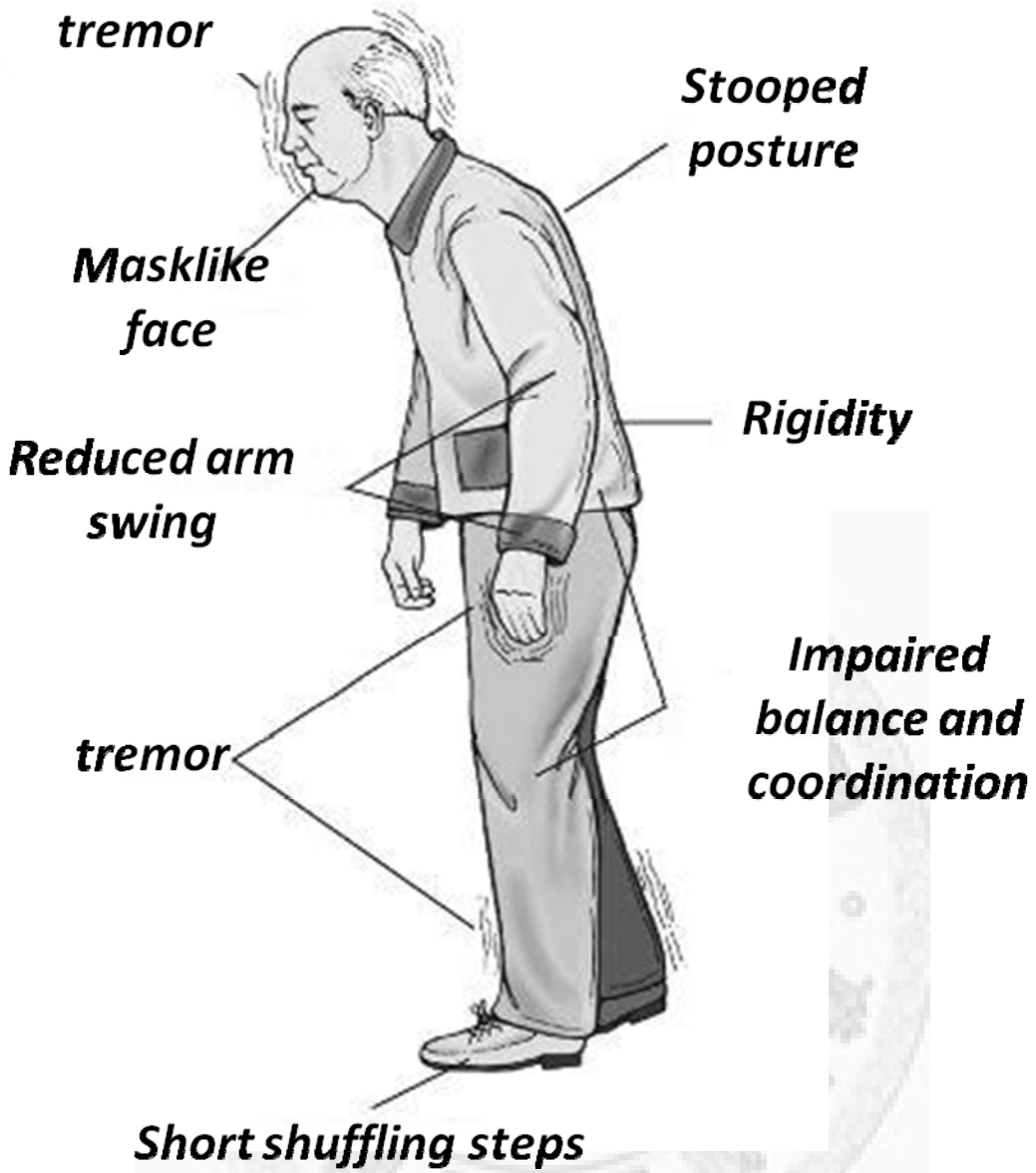

Figure 1.2 Clinical signs of Parkinson's disease include tremor, stooped posture, masklike face, rigidity, impaired balance and coordination, and short shuffling steps. (from [7])

Resting tremor is an involuntary oscillation of a body part occurring at rest, with a rate of 4 to 7 oscillations per second [8, 9]. Rigidity is a major clinical sign of PD and patients with PD often complain of "heaviness" and "stiffness" of their limbs [8]. Impaired balance reaction is also observed in PD patients. With the loss of balance and postural stability, PD patients typically experience difficulty in maintaining upright balance, walking, or turning around [10]. PD patients therefore fall easily [11, 12] and are threatened by fracture and consequent lengthy hospitalization

[13]. Bradykinesia means “slowness” of movement, PD patients frequently have difficulty in initiating movement [8]. Both the voluntary and automatic movements are reduced in speed, range, and amplitude, indicating termed “freezing” of movement [8].

Because overall coordination is impaired, PD patients with bradykinesia cannot perform fine tuning in motor tasks such as writing or grasping small objects. Poverty of movement commonly affects PD patients and involves an overall decrease in the total number of movements. PD patients are often unable to perform two different movement tasks at the same time or to combine motor programs into complex sequences.

1.1.3 Gait disorders as cardinal motor symptoms in early stages

Although the clinical presentation and progression can be greatly variable, gait disturbance presents a cardinal motor symptom and may be observed in early stages of the disease. With a generalized lack of extension at hip, knee, and ankle joints, PD patients walk with a slow and shuffling gait [14-16], and reduced reciprocal arm swing [17]. A festination (propulsion) gait may occur due to a forward flexed or stooped posture when walking [18].

1.2 Gait analysis

Gait analysis is the systematic study of human locomotion. Acquisitioned and augmented by instrumentation and sensors, kinetic and kinematic parameters, including joint angular velocity, acceleration, inertia force, ground reaction force, speed, gait cycle duration, and even muscle activity during locomotion, are quantified and analyzed to obtain productive information that helps

us understand the nature of gait. Clinically, gait analysis helps the medical staff (e.g. clinicians and physic therapists) to assess, plan, and treat patients with neural or physical injuries that affect their ability to keep balance and posture during walking.

1.2.1 Computer-aided video gait analysis

With the availability of video camera systems in the 1970s, the widespread application of gait analysis surged as a vigorous course [19-22]. Development of microelectronics speeds up the innovations of the modern computers. With the assistance of modern powerful computers, video-based motion analysis has become a popular solution for gait analysis [19-24] in the past decades. Researchers were able to observe and demonstrate the gait of patients with PD and other pathological conditions such as cerebral palsy, stroke, and neuromuscular disorders within realistic cost time constrains, definitely. Instead of traditional evaluations conducted by human inspectors, researchers currently use computer-aided video gait analysis for precise data collection, reliable quantitative measurements, and systematic data management. As natural body movements can be transformed into essential spatial-temporal parameters with video-image analysis, abnormalities in gait and posture can be captured and identified with precision [25-27].

1.2.2 Requirements of available computer-aided video gait analysis

Commercial motion analysis systems, including the Vicon Motion Systems and BTS (Vicon Inc., Oxford, UK), which are performed using a setup consists of floor-mounted load transducers,

high-powered strobes, LED, and sensors placed onto particular body regions, facilitate clinical treatment regimes and follow-up monitoring. A typical modern gait lab is presented as Figure 1.2.

Figure 1.3 A gait laboratory with lighting condition, passive infrared cameras, and embedded force platforms

There are several cameras placed around a walkway or treadmill, which are connected to a console computer. Subjects participating in gait trials are asked to have single markers applied to palpable bony landmarks, such as the iliac spines of the pelvis, the malleoli of the ankle, and condyles of knee. The subjects then will be instructed to walks down the walkway or the treadmill and the console computer will record data from cameras to calculate the moving trajectories of single markers in three dimensions. A full breakdown of the motions at each joint is given through a model that is applied to compute the underlying motion of the bones.

1.3 Purpose of this study

The recognition and evaluation of the progression of PD in the early stages are important issues in treatment and care for PD patients. The available commercial motion analysis methods provide accurate kinematic measurements of the parkinsonian gait [6] and other neuromuscular disorders [28-31]. However, an experimental setup consisting of a wide stage, force plates, multiple infrared cameras, reflective balls, light-emitting diodes (LED), or inertial sensors placed onto regions of the subject's body are demanded [32]. Furthermore, dedicated manpower is required to calibrate the camera system, apply the reflective balls, and utilize the software. These properties of conventional gait analysis limit its application in many clinical settings, such as clinics with space or budgetary limitations. Thus a method for performing gait analysis that can be applied in clinics within a limited space to identify PD patients and determine the therapeutic effect of drug management on PD is required. To provide a solution that can be easily installed and used in a clinic or at home to monitor and quantify the spatial-temporal gait parameters, we propose a portable system to track and analyze parkinsonian gait in this study.

1.4 The hypotheses of the proposed study

Herein, we introduce two hypotheses of the proposed study and thereby set the stages for the following research. The details of the two hypotheses will be reiterated in chapter 3 and 4, respectively.

Hypothesis 1: The walking silhouette contributes to the identification of different gaits. Therefore the mild parkinsonian gait in the different states can be identified from the monocular image sequences using a feature-based method.

Hypthesis 2: The gait initiation and symmetry are deteriorated in the early stages of Parkinson's disease. Thus, it is possible to identify the parkinsonian gait from the monocular image sequences using a method that analyzes the gait performance and symmetry during the gait initiation period.

1.5 Overview of the dissertation

The primary goal of this research is to provide a portable system to quantify the parkinsonian gait. Using the solution, researchers and clinicians with space or budgetary limitations are able to recognize the mild PD gait and quantify the improvement from medical treatment and care. This dissertation comprises chapters as follows:

Chapter 1 provides a brief overview of Parkinson's disease and the computer-aided video motion analysis method, and the demonstration of the incentive to begin the research.

Chapter 2 provides descriptions of two methods developed to enhance the portable system utilizing the monocular image sequences of walking to acquire quantitative analysis of mild parkinsonian gait performance during the gait initiation and steady-state walking periods and associated symmetry indexes.

Chapter 3 describes a video-based method with simple clinical setting uses the KPCA to

quantify and recognize mild parkinsonian gait during the steady-state walking period at clinics with space and budgetary limitations. We hereby prove the hypothesis 1.

Chapter 4 presents the second gait analysis method, the centroid tracking algorithm (CTA), to provide an approach with demand for less space and budget. The CTA shows that the mild parkinsonian gait has more significant difference in the performance and walking symmetry during the gait initiation period than those during the steady-state walking period when comparing to the healthy subjects. We hereby prove the hypothesis 2.

Chapter 5 provides a summary of the key findings, conclusions that were drawn, and follow-up recommendation for future studies.

Chapter 2 Parkinsonian gait analysis using monocular image sequences

2.1 The silhouette-based parkinsonian gait analysis method

To establish a portable system that can be easily installed and used in a clinic to do parkinsonian gait analysis, the quite simple clinical setting and the easy-to-use portable equipment are required. The silhouette method provides an economical solution for gait identification in clinical settings [33]. Requiring only a monocular digital camera to capture the silhouettes of the subjects walking, the method largely reduces the computational cost and storage size; the image processing procedures are also simplified [34]. As a lower-cost method that requires less space and less dedicated manpower than the Vicon motion analysis method based on model reconstruction, the existing approaches that utilize walking silhouettes perform well in recognizing different gaits [35-38]. However, the quantitative measurements of the gait parameters are not provided. To quantify the abnormalities in mild parkinsonian gait, the kernel-based principal component analysis (KPCA) [39] is developed in the 1st part of this research to enhance the simple and efficient silhouette method.

2.2 The kernel principal component analysis

The KPCA is an extension of known Principal Component Analysis (PCA) [37, 40] that is a powerful technique and widely utilized in image processing [41-45] and data classification [46-49].

The PCA is an eigenvalue decomposition procedure that uses an orthogonal linear transformation to transform a set of possibly correlated input variables into a new coordinate system and acquire a set of uncorrelated variables called principal components. A simple and concise description of the PCA is as the following.

The PCA procedure begins at acquiring the covariance matrix of a multi-dimensional dataset. For example, for a ***N*** dimensional dataset $\boldsymbol{X} = [x_1, x_2, ..., x_n]$, we can derive $n!/(2(n-2)!)$ different covariance values. The next step is to derive the eigenvalues of the covariance matrix and sorted them as $\lambda_1 \ldots \lambda_n$, the highest to lowest, and the corresponding orthogonal eigenvectors $e_1 ... e_n$ once the covariance matrix is derived, wherein $e_i^{'} \times e_i = 1$ and $e_i^{'} \times e_j = 0$. The ***N*** dimensional dataset ***X*** then can be decomposed into ***n*** orthogonal (uncorrelated) vectors as the following,

$$y_i = e_i^{'} \boldsymbol{X} = e_{i1} x_1 + e_{i2} x_2 + ... + e_{in} x_n \qquad i = 1, 2, ..., n \tag{2.1}$$

wherein $y_1 \ldots y_n$ are principal components of the ***N*** dimensional dataset ***X***, and therefore form a new coordinate system. To be noted, the number of principal components must be less than or equal to the number of original variables. The eigenvector corresponding to the greatest eigenvalue (also indicating the greatest covariance) by the orthogonal linear transformation of the ***N*** dimensional dataset comes to lie on the 1st coordinate (called the 1st principal component), the eigenvector with the 2nd greatest eigenvalue (also indicating the 2nd greatest covariance) on the 2nd coordinate, and so on. After all of the principal components are determined, we can keep the components corresponding to more significant eignevalues and leave out the ones corresponding to smaller eigenvalues, indicating that we can describe the original data with reduced dimensions. A

multi-dimensional dataset with the 1st and the 2nd principal components y_1 and y_2 are presented as **錯誤! 找不到參照來源。**.

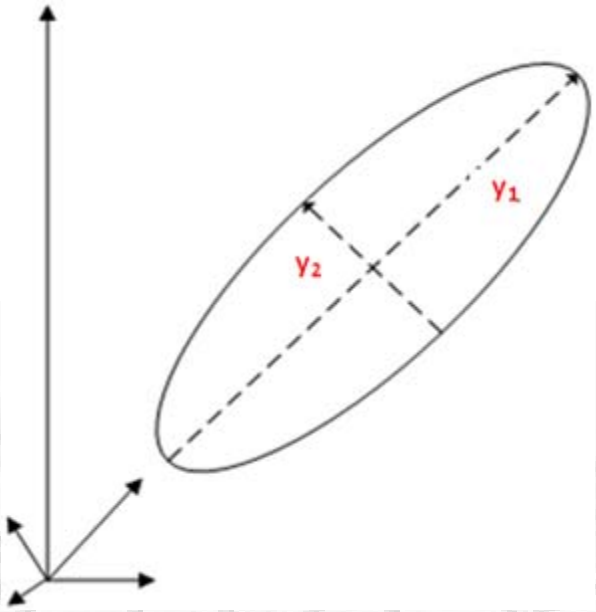

Figure 2.1 The 1st and the 2nd principal components y_1 and y_2 of a multi-dimensional dataset

However, many data types implicitly contain non-linear structures and principal variable components, which are nonlinear and related to the input variables. KPCA is an extension of PCA that uses kernel methods [50] to extract the nonlinear components. In recent years, KPCA has been suggested for various image-processing tasks, such as image noise reduction and compression, as PCA is used to decompose linear combinations of data sets and does not reflect the generation process of natural images [51]. The following is a brief introduction to KPCA.

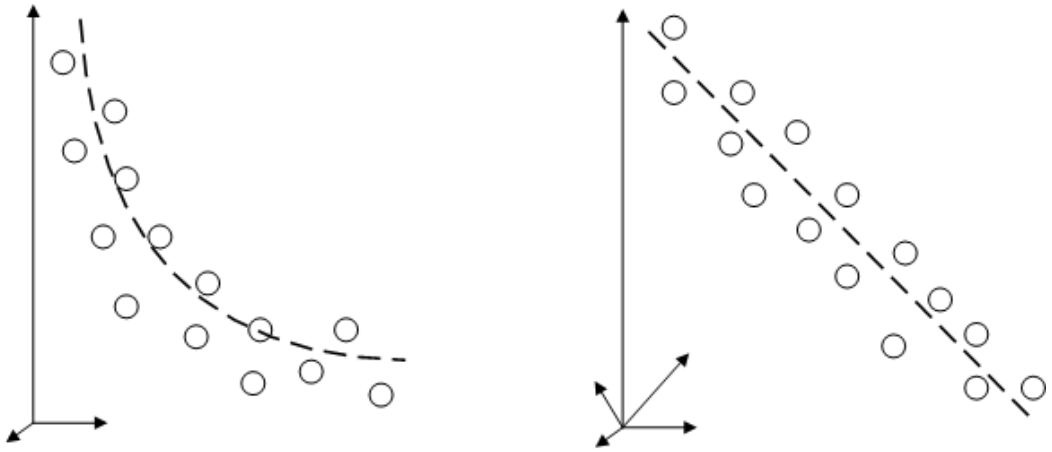

Figure 2.2 (a) a non-linear structure of dataset (b) a linear structure of dataset

Consider space *X* with a set of *N* vectors, $x_1, x_2, \cdots, x_N$, which encompasses a set of an *N*-dimensional vector (for example, *N* = 64 × 64 = 4096 from a trimmed binary silhouette captured in chapter 3). To analyze the nonlinear components of *X*, the covariance matrix *C* that contains the nonlinear principal components can be acquired by mapping *X* to a feature space, *H*. The mapping equation (2.2) is shown below.

$$C = \frac{1}{N}\sum_{j=1}^{N} \tilde{\varphi}(x_j)\tilde{\varphi}(x_j)^T \tag{2.2}$$

$$\tilde{\phi}(x_i) = \phi(x_i) - m^{\phi} \tag{2.3}$$

$$m^{\phi} = \frac{1}{N}\sum_{i=1}^{N}\phi(x_i) \tag{2.4}$$

where $\phi(x_i)$ is a nonlinear polynomial function that maps the vectors to *H*, x_j is the *j*-th vector, *N* is the total number of vectors, *T* contains the centralized mapped data of the transposed matrix, m^{ϕ} is the mean, and $\tilde{\phi}(x_i)$ is the centralized mapped data with m^{ϕ}. To acquire the eigenvector, *v*, and eigenvalue, λ, of the covariance matrix, *C*, the following equation must be solved:

$$\lambda v = Cv \tag{2.5}$$

Because $\tilde{\varphi}(x_i)$ is a vector with approximately infinite dimensionality, it is difficult to solve the covariance matrix, *C*. Therefore, a new $N \times N$ centralized kernel matrix, $\tilde{K}$, is defined to acquire the eigenvector and eigenvalue of *C*.

$$\tilde{K} = \tilde{\varphi}(x_i) \cdot \tilde{\varphi}(x_j) = K - l_N K - K l_N + l_N K l \tag{2.6}$$

$$K_{ij} = \phi(x_i) \cdot \phi(x_j) = k(x_i, x_j) \tag{2.7}$$

$$k(x_i, x_j) = (x_i \cdot x_j)^d, \quad d > 1 \tag{2.8}$$

$$(l_N)_{ij} = \frac{1}{N} \tag{2.9}$$

where *i* and *j* are the indices of the row and column, respectively, of vector *x*, $k(x_i, x_j)$ is a polynomial kernel function for acquiring the dot product of the vectors from the original space and $d > 1$ because the result of KPCA is identical to that obtained from PCA, where $d = 1$. The relationship between the eigenvector, $\tilde{v}$, of the kernel matrix, $\tilde{K}$, and the eigenvector, v, of the covariance matrix, *C*, can be expressed as

$$v_k = \frac{1}{\sqrt{\tilde{\lambda}_k}} Q \tilde{v}_k, k = 1, 2, \cdots, \mathrm{m} \tag{2.10}$$

$$Q = [\tilde{\varphi}(x_1) \tilde{\varphi}(x_2) \cdots \tilde{\varphi}(x_N)] \tag{2.11}$$

where $\tilde{\lambda}_k$ is a nonzero set of eigenvalues of $\tilde{v}$, *m* is the number of non-zero eigenvalues and Q is a centralized mapped data set. After projecting *Q* to the feature space constructed by $v_1, v_2, \cdots, v_m$, the k^{th} KPCA feature vector, y_k, can be represented as

$$y_k = v_k^T Q = \frac{1}{\sqrt{\tilde{\lambda}_k}} \tilde{v}_k^T Q^T Q = \frac{1}{\sqrt{\tilde{\lambda}_k}} \tilde{v}_k^T \tilde{K} \tag{2.12}$$

where *T* refers to the transposed matrix.

To summarize, the KPCA computation can be separated into three steps. The first step is to determine parameter d in (2.8) for the polynomial kernel function and derive kernel matrix $\widetilde{K}$ according to equation (2.6). The second step is to derive the k^{th} major eigenvector, $\tilde{v}_k$, of the $N \times N$ centralized kernel matrix, $\widetilde{K}$, and acquire the k^{th} coordinate vector, v_k, using equation (2.10). The third step is to project the centralized mapped data set, Q, to the feature space using equation (2.12) and to acquire the k^{th} KPCA feature vector, y_k.

2.3 The quantitative analysis of parkinsonian gait initiation and symmetry

Amongst the clinical signs of parkinsonian gait pattern, the disordered gait initiation [6, 52, 53] and gait asymmetry [54, 55] represent the major symptoms in the early stages of this disease and are commonly used to identify the gait of and evaluate the gait performance of patients with mild PD besides the affected gait parameters during the steady-state walking.

Gait initiation is defined as a task that challenges the balance control system by requiring a transition from motionless and stable standing to continuous unstable steady-state locomotion, also indicating from double- to single-leg stances [6]. Due to bradykinesia, PD patients require longer motor preparation time than healthy individuals and perform a hesitation and freezing when initiating gait. Their feet appear to be stuck on the floor, indicating that the ability to generate a normal gait pattern is impaired [56].

Gait symmetry is defined as a task to coordinate actions between the right and left lower limbs and behave the actions identically to produce rhythmical motion during walking [57]. Due to the

predominantly unilateral occurrence of tremor, rigidity, and bradykinesia, PD patients present the dysfunction at coordinating their lower limbs and motor deficiency [58]. As results, PD patients walk slowly and their steps are small. Their stride and step lengths [59, 60], velocity profiles [61, 62], and ranges of joint motion [63] reduce because different behaviors between the two lower limbs.

Although the KPCA that is proposed to enhance the silhouette-based method may provide quantitative analysis of mild parkinsonian gait during walking, the left and right sides of participants cannot be identified in binarized monocular image sequences. Therefore the information concerning the gait symmetry is not provided in the 1st part of this study. To acquire the quantification of gait symmetry during walking by a digital camera, in the 2nd part of this study, a method using the centroid tracking algorithm (CTA) is developed to track joint identifiers secured on palpable landmarks of left and right lower limbs during walking, by which a number of quantitative gait parameters and associated symmetry indexes during the gait initiation and steady-state walking periods are assessed for providing a complete evaluation of the mild PD gait performance.

2.4 The centroid tracking algorithm (CTA)

The centroid tracking algorithm (CTA) is a method used to track a moving object [64]. Basically, the CTA captures the centroid of a moving object of interest within an image frame sequence, and then records the centroid moving trajectory of the object of interest. The CTA is

independent of the size of targets and less sensitive to the intensity of the targets because the motion recognition characteristics of a target of interest are its location, velocity, and acceleration, which are obtained using data from successive image frames. If the target size is known, the CTA may set limits for removing the clusters that differ sufficiently from the size of the target cluster in a same image frame to reduce the computational complexity [65].

The flow chart of the CTA is illustrated in Figure 2.3 and the procedure details are the following.

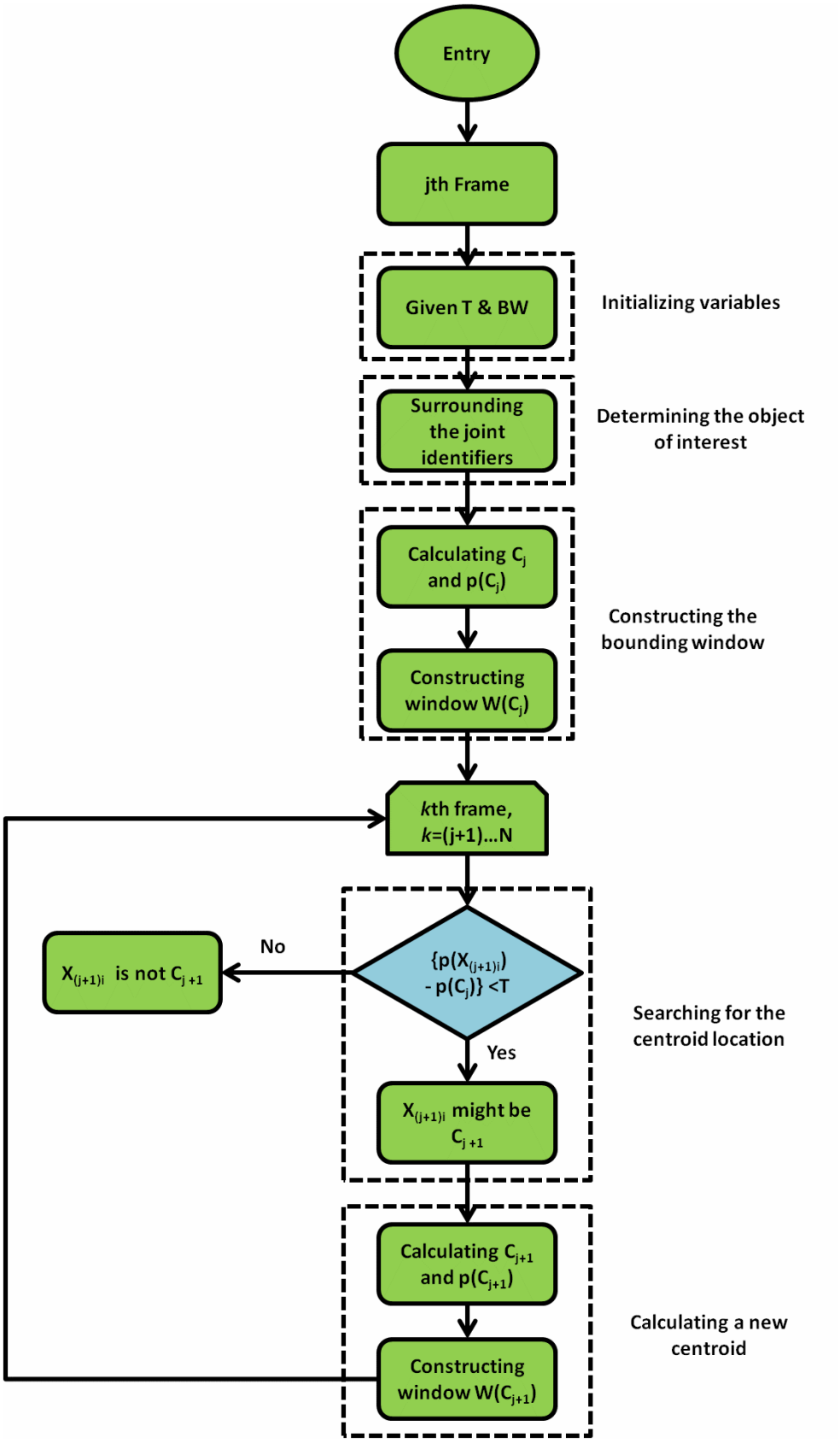

Figure 2.3. The flow chart of the centroid tracking algorithm.

Step 1. Initializing variables

Two important variables, the tolerating pixel value ***T*** and the bounding window size ***BW*** are initialized. ***T*** and ***BW*** are used to reduce the searching range and tolerate light influences on the tags depending on the size of two markers put on the fibula head and lateral malleolus. In this study, ***T*** and ***BW*** are set as constants 10 and 5 in all sequences, respectively.

Step 2. Determining the object of interest

The object is selected from the *j*th frame. The centroid location C_j is calculated from a set $\{x_{(j)i}\}_{i=1\ldots n}$, where $x_{(j)i}$ represents the location of the chosen object, *n* is the number of pixels in the chosen object, and $p(C_j)$ is the pixel value of C_j.

Step 3. Constructing the bounding window

A rectangular window $W(C_j)$ with a center C_j is constructed as the searching region for the *j*th frame. The centroid C_j is defined as:

$$\{C_j(x), C_j(y)\} = \{median(x_{(j)i}(x)), median(x_{(j)i}(y))\}_{i=1\ldots n} \tag{2.13}$$

The bounding window $W(C_j)$ of frame *j* is defined as:

$$W(C_j) \in \begin{pmatrix} \{[C_j(x)-\boldsymbol{BW}],[C_j(y)-\boldsymbol{BW}]\} & \{[C_j(x)-\boldsymbol{BW}],[C_j(y)+\boldsymbol{BW}]\} \\ \{[C_j(x)+\boldsymbol{BW}],[C_j(y)-\boldsymbol{BW}]\} & \{[C_j\{x\}+\boldsymbol{BW}],[C_j(y)+\boldsymbol{BW}]\} \end{pmatrix} \tag{2.14}$$

An orange cross presents the centroid C_j and an orange rectangle presents the bounding window $W(C_j)$ are shown in Figure 2.4(a).

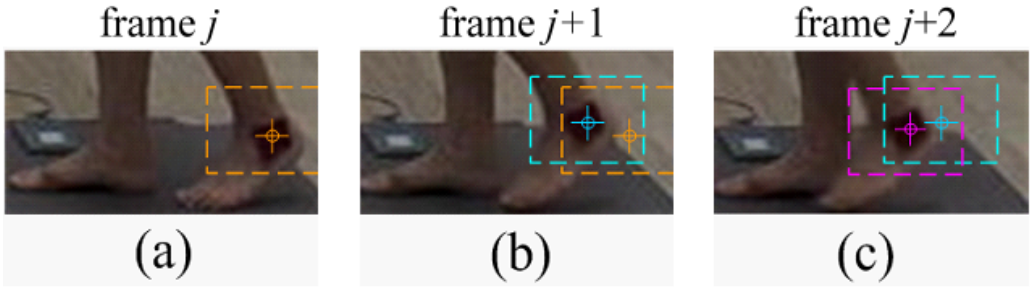

Figure 2.4. The centroid tracking algorithm used to determine the centroid (color crosses) and the bounding window (color rectangle) in each frame.

Step 4. Searching for the centroid location.

As illustrated in Figure 2.4(b), all pixel values within the orange rectangle in (*j+1)*th frame subtract the $p(C_j)$ that is the pixel value of the C_j, the centroid of the object of interest appears in the *j*th frame. If the subtraction is smaller than the tolerating pixel value ***T***, these locations $x_{(j+1)i}$ are considered as candidates for the centroid location $C(x_{(j+1)i})$ in the (*j+1)*th frame, as represented by the following equation:

$$\begin{aligned} &x_{(j+1)i} \in C(x_{(j+1)i}), && \text{if} \quad p(x_{(j+1)i}) - p(C_j) \le \boldsymbol{T} \\ &x_{(j+1)i} \notin C(x_{(j+1)i}), && \text{otherwise} \end{aligned} \tag{2.15}$$

Step 5. Calculating the new centroid.

After the locations $x_{(j+1)i}$ in $C(x_{(j+1)i})$ are acquired, a new centroid location C_{j+1} is calculated by averaging $x_{(j+1)i}$. Subsequently, the new bounding window $W(C_{j+1})$ with the new centroid location C_{j+1} is determined. The centroid C_{j+1} and the bounding window $W(C_{j+1})$ of the (*j+1)*th frame are presented as the cyan cross and cyan rectangle in Figure 2.4(b). Finally, steps 3 to 5 were repeated to determine the centroids of the moving within all image frames and then determine a moving trajectory of the object of interest in an image frame sequence. The centroid C_{j+2} and the bounding window $W(C_{j+2})$ of (*j+2)*th frame are presented as the violet cross and

violet rectangle in Figure 2.4(c).

The CTA adopts the concept of the kernel function to create a bounding window as a search region; the locations in which the searched pixel value is more similar to the pixel value of the region of interest are identified. A new centroid location is then computed to represent the current object. By adjusting the size of the bounding window according to different states, sudden changes in the direction of the object can be tolerated, resulting in a simple and accurate tracking method.

Chapter 3 Quantification and recognition of parkinsonian gait using kernel principal component analysis

3.1 Background and motivation

Hypothesis 1: The walking silhouette contributes to the identification of different gaits. Therefore the mild parkinsonian gait in the different states can be identified from the monocular image sequences using a feature-based method.

As gait disorders are symptoms of the early stages of PD, gait performance has become a specific and major hallmark in the recognition of patients with mild PD and the evaluation of the progression of the disease [28, 52, 66]. The Unified Parkinson's Disease Rating Scale (UPDRS, please refer to **Appendix A** for a more detailed description) [67] is widely used to assess and track the longitudinal course of PD. It is also used to evaluate the level of motor impairment and response to medical treatment, such as levodopa (L-dopa, please refer to **Appendix A** for a more detailed description), for PD patients. However, such evaluations rely on the experience and/or the expertise of the clinician. Observations based on the UPDRS part III, for evaluation of motor impairment, tend to be subjective. In light of the issues mentioned, a quantitative measurement for parkinsonian gait is much needed.

In order to provide a simple and efficient solution for the quantification and recognition of parkinsonian gait, a video-based silhouette method using kernel-based principal component analysis (KPCA) [39] is developed in this study. The aim of the approach is to provide clinicians and researchers with an easy-to-use and –install tool to recognize and quantify the gait performance of non-PD subjects and patients with mild PD in both "Drug-Off" and "Drug-On" states. Participants' gait patterns during the steady-state walking period is captured using the proposed approach. Temporal and spectral analyses of gait patterns are investigated. The correlations

between the UPDRS part III scores used to assess motor impairment and the kinematic gait parameters extracted by the proposed method are also inspected.

3.2 Methods

3.2.1 The participants

Twelve patients with mild PD who scored an average rating of 2.33 on the Hoehn and Yahr (H&Y) scale (six scored 2.5, five scored 2, and one scored 3) and twelve healthy adults with no neurological history that might cause motor disorders within the past six months were recruited from Hualien Buddhist Tzu Chi General Hospital, Taiwan. The subjects volunteered to participate, and informed consent was obtained from all subjects in accordance with Buddhist Tzu Chi General Hospital's Institutional Review Board (IRB 097-08) Committee on research involving human subjects. The biometric characteristics of the participants are listed in table 3.1. The healthy adults were denoted as non-PD subjects; the patients with mild PD given L-dopa at an equivalent daily dose for one hour were classified as "Drug-On", whereas those that abstained from L-dopa treatment for at least 12 hours were classified as "Drug-Off". For the patients with mild PD, the degree of motor function impairment was evaluated using part III of the UPDRS.

Table 3.1 The basic biometric characteristics of categorized subjects.

	PD group (9M/3F)			non-PD group (3M/9F)		
	Min	Max	Mean±SD	Min	Max	Mean±SD
Age (years)	49.00	74.00	60.30±6.71	48.00	67.00	56.40±7.04
Height (m)	1.50	1.82	1.52±0.46	1.49	1.80	1.60±0.08
Weight (kg)	36.00	106.00	63.05±24.37	50.00	67.00	58.08±5.05
Body mass index (kg/m^2)	13.38	36.25	24.90±5.74	21.36	24.37	22.76±1.15
Disease duration (years)	1.00	18.00	8.00±4.82	N/A	N/A	N/A
Hoehn and Yahr stage	2	2.5	2.33±0.33	N/A	N/A	N/A

SD = standard deviation

3.2.2 Environmental setup and videotaping standard

A 6-m corridor decorated with a navy curtain was prepared for the walking trials. A commercial digital charge-coupled device (CCD) video camera (PV-GS400, Panasonic) was mounted on a

tripod and placed 4.1 m in front of the curtain, perpendicular to the walking pathway, to capture the lateral view of each participant's walk.

All participants were asked to wear clothing of a much lighter color than the curtain to facilitate the filtration of noise during image post-processing. To reduce the variability of the gait performance, the participants were asked to perform three walking trials. All participants were asked to walk at their natural pace in order to naturally reflect their gait performance. Between trials, the participants were instructed to rest for at least five minutes until their strength was recovered.

The patients with mild PD were asked to abstain from L-dopa overnight for at least 12 hours prior to the gait measurements. They then performed three drug-off trials in the morning. Immediately following the completion of the drug-off trials, they were given L-dopa at an equivalent daily dose. Three drug-on trials were then assessed one hour after the administration of L-dopa.

In this study, we utilized the participant's gait performance during the steady-state walking period to assist in the verification of the proposed method. Therefore, the participants were asked to begin walking 2 m from the left end of the corridor. Moreover, the last 1 m of each walking period was not videotaped so that patient deceleration did not affect the data.

The experimental setup and the flowchart of the data analyses are illustrated in Figures 3.1 and 3.2, respectively.

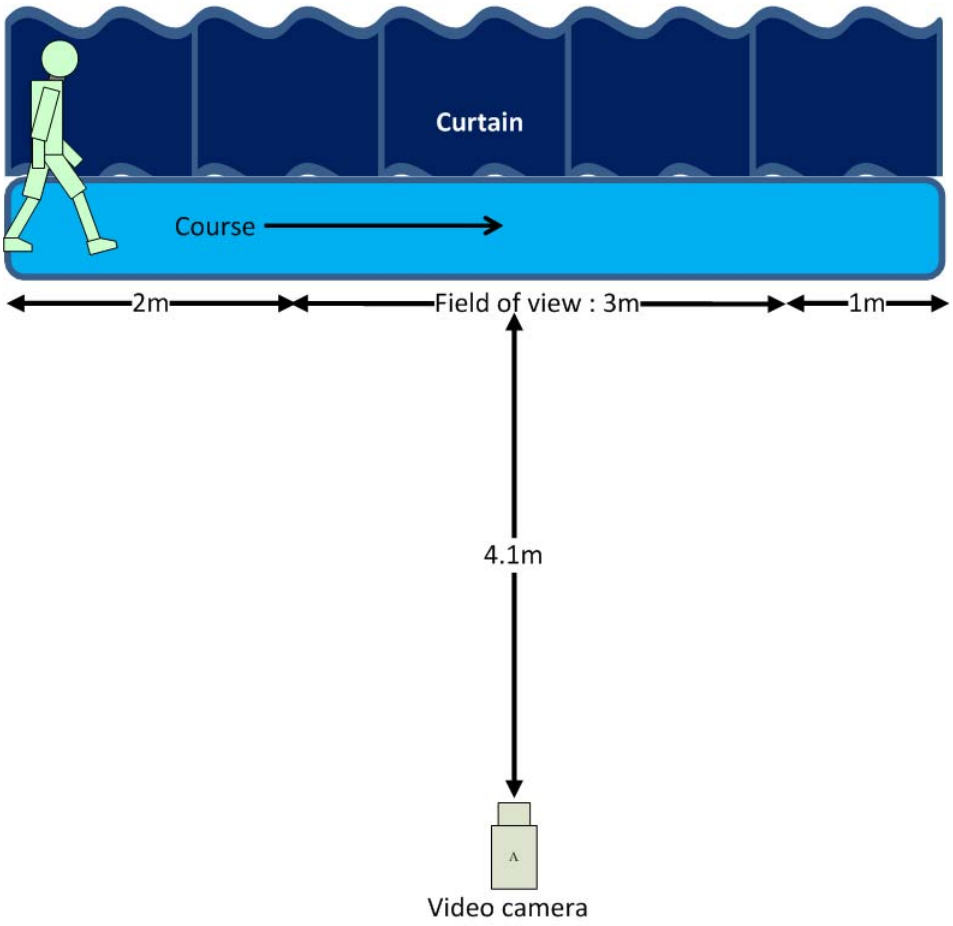

Figure 3.1 A general schematic of the experimental setup used for video recording. The participant wears a light suit to enhance the contrast between the individual and the dark background. The participant walks along the course (approximately 6 m) in front of the video camera (located approximately 4.1 m away). To ensure that the captured data reflect the gait performance during the steady-state walking period, the camera videotapes only the middle 3 m of each walking trial.

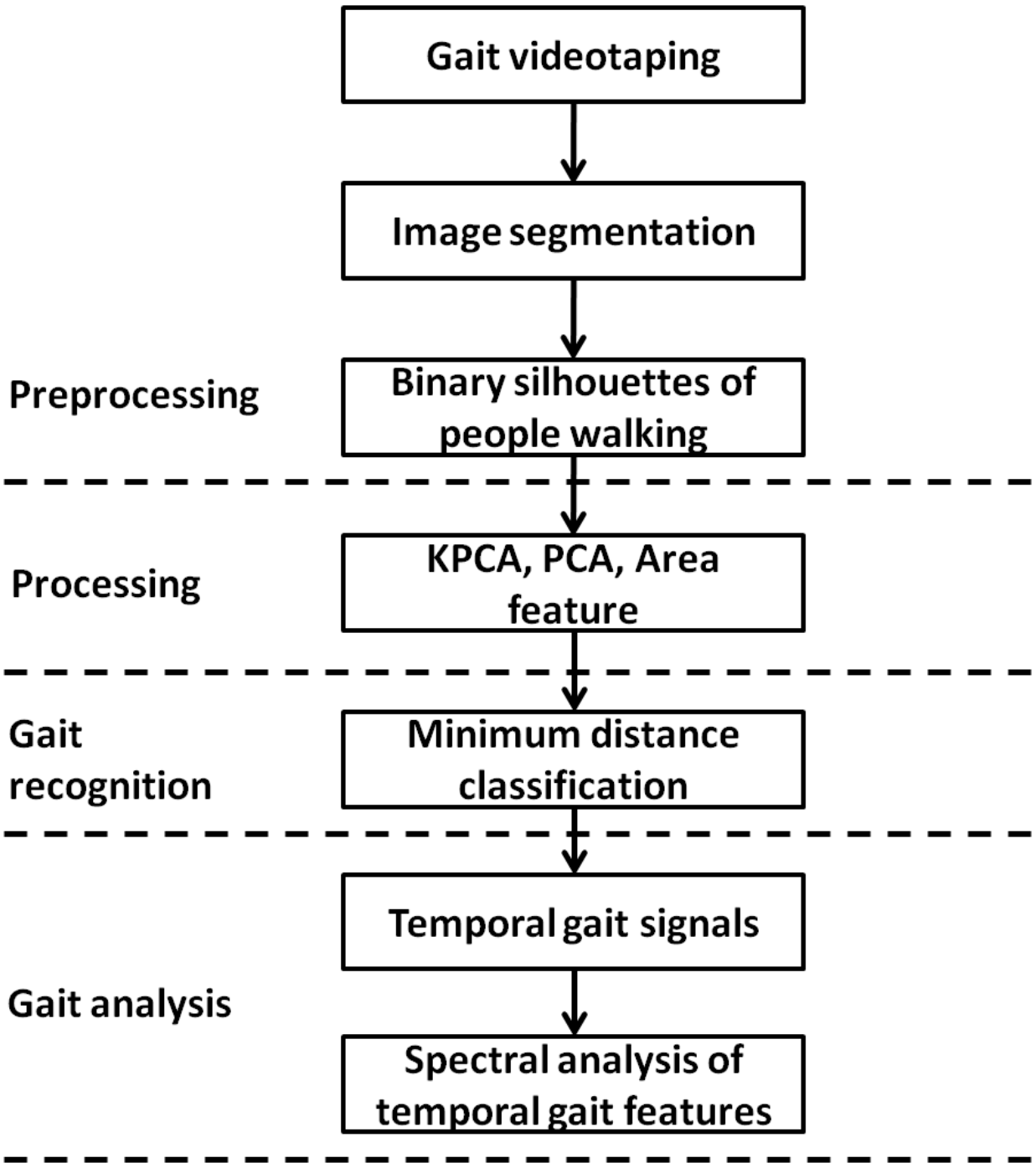

Figure 3.2 A flow-chart of gait analysis and recognition.

All trials were videotaped using a sampling rate of 15 image frames per second and an image size of 320 × 240 pixels. The spatial resolution was approximately 1.06 pixel/cm. The video files were segmented and separated into sequential images. Using the method and equations presented in **3.2.4 binary silhouettes collection**, the background of the sequential images can be removed, and the processed sequential images can be transformed into binary images that represent the walking

silhouettes to facilitate image noise reduction. Each sequential binary image is then transformed into an encoded one-dimensional matrix containing the biometric features of the gait. KPCA is then applied to detect the biometric features. Using KPCA, the walking silhouettes can be decomposed, and the biometric features of the people walking can be extracted for gait analysis. The efficiency of the KPCA-based feature approach was compared with other competing methods, the area [68] feature approach and the principal component analyses (PCA) [37, 40]-based feature approach. To this end, the minimum distance classifier (MDC) [69, 70], a numerical approach, was used to classify the different gaits and determine the classification sensitivity. The discrete Fourier transform (DFT), which is used to transform a signal in the time domain into a representation in the frequency domain, was applied to transform the coefficients of the KPCA components to understand the spectral power distribution of the different gaits. The KPCA, MDC, and DFT algorithms and the data analysis were implemented using MATLAB (MathWorks, Natick, MA) on a personal computer. The details of implementing the KPCA, MDC, and DFT algorithms for parkinsonian gait analysis are described in KPCA-based feature extraction and heel strike determination, minimum distance classifier (MDC) for classification, and spectral analyses for temporal gait feature signals, respectively. In our preliminary experiments, the KPCA-based feature approach was tested on six healthy adults and compared to the GAITRite® system (CIR system, Inc., USA) for validation. The preliminary results showed that there was no difference in assessing the kinematic gait parameters of interest, indicating that the KPCA-based feature approach was an easy-to-use and inexpensive tool for measuring the selected kinematic gait parameters. We were convinced of the validity of the KPCA-based feature approach in assessing the gait performance of adults and continued to use it to assess the kinematic gait parameters of the participants in the present study. Detailed descriptions for the setup of the preliminary experiment and the translation of the results are presented in **Appendix B**.

3.2.3 Background Construction

Because we were interested in the silhouette data of a participant walking, the invariant background scene was unnecessary for further gait analyses and should be discarded. The intensity median value of each pixel, which is at the same location through an entire gait sequence, was utilized to construct the background image and is represented as the following:

$$\mathbf{B}(i,j) = \text{median}_{\mathbf{TN}}\left(\mathbf{I}_t(i,j)\right) \tag{3.1}$$

where $\mathbf{I}_t(i,j)$ is the brightness at location (i,j) in the specific image that corresponds to time instant t. **TN** is the total number of images in the entire sequence, and $\mathbf{B}(i,j)$ is the background pixel value.

3.2.4 Binary silhouette collection

To separate the silhouettes from the image frames of the patient walking, the background images for each videotaped gait sequence are prepared using equation (1). A silhouette pixel of the patient walking is acquired by the difference method from [71], represented as equation (2).

$$\mathbf{F}_t(i,j) = 1 - \frac{2\times\sqrt{\left(\mathbf{I}_t(i,j)+1\right)\left(\mathbf{B}(i,j)+1\right)}}{\left(\mathbf{I}_t(i,j)+1\right)+\left(\mathbf{B}(i,j)+1\right)} \times \frac{2\times\sqrt{\left(256-\mathbf{I}_t(i,j)\right)\left(256-\mathbf{B}(i,j)\right)}}{\left(256-\mathbf{I}_t(i,j)\right)+\left(256-\mathbf{B}(i,j)\right)} \tag{3.2}$$

$$\boldsymbol{THR} = \frac{1}{\boldsymbol{M}}\sum\frac{\boldsymbol{B}(i,j)}{256} \tag{3.3}$$

$$\begin{cases} \mathbf{F}_t(i,j) = 1, & if\ \mathbf{F}_t(i,j) > \boldsymbol{THR} \\ \mathbf{F}_t(i,j) = 0, & if\ \mathbf{F}_t(i,j) < \boldsymbol{THR} \end{cases} \tag{3.4}$$

where $\mathbf{I}_t(i,j)$ is the brightness intensity of a pixel (i,j) in a particular image frame at an instant t, $\mathbf{B}(i,j)$ is the brightness intensity of a prepared background image pixel, $\boldsymbol{M}$ is the total number of the pixels within the prepared background image (in this case, $\boldsymbol{M}$ = 320 × 240) and $\boldsymbol{THR}$ is the threshold used to separate a walking silhouette from the original gait sequential image frame. According to equation (3.3), the brightness levels of all of the prepared background image pixels is

averaged and normalized to determine the threshold ***THR,*** ranging from [0, 1]. According to equation (3.4), if $\mathbf{F}_t(i,j)$, the brightness level of a silhouette pixel, > ***THR***, $\mathbf{F}_t(i,j) = 1$; if $\mathbf{F}_t(i,j) <$ ***THR***, $\mathbf{F}_t(i,j) = 0$. After the binarized procedure, 320 × 240 pixel binary silhouette image frames are acquired. The 320 × 240 pixel binary silhouette image frames are then trimmed to 64 × 64 pixels to preserve the walking silhouette, eliminate redundancies, and reduce the computational costs during image analyses. An example of gait image processing is represented in Figure 3.3. The trimmed binary silhouettes of the sequential walking image frames from the non-PD subject and mild PD patient in the "Drug-Off" and "Drug-On" states are illustrated in the top region and middle and bottom regions in Figure 3.4, respectively.

Figure 3.3 An example of gait image processing: top: original color image frames, bottom: binary silhouette frames.

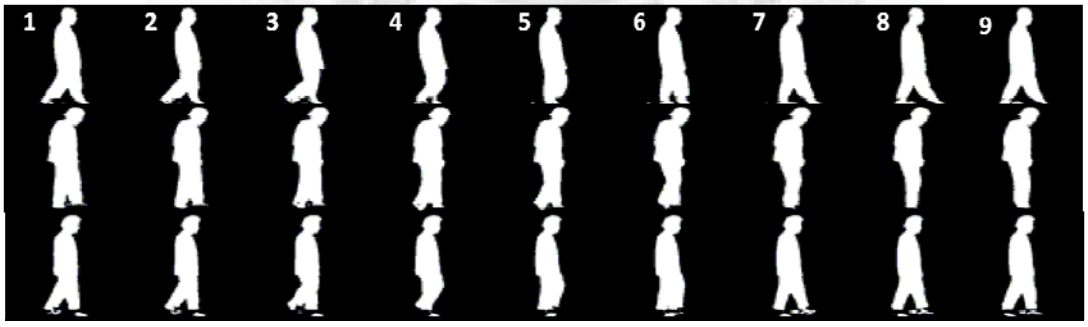

Figure 3.4 The trimmed 64 × 64 pixel binary walking sequence silhouettes of a non-PD subject (top) and a patient with mild PD in the "Drug-Off" (middle) and "Drug-On" (bottom) states.

3.2.5 KPCA-based feature extraction and heel strike determination

Modern advances in computing power have greatly widened researchers' scope in gathering

and investigating information from many variables, information which might have been ignored in the past. Yet to effectively scan a large pool of variables is not an easy task, although the ability of researchers to interact with data has been much enhanced by recent innovations in dynamic graphics. In this study, KPCA is used to reduce the dimensionality of image frames with multiple nonlinear components. After projecting the centralized mapped data set Q, the k^{th} KPCA feature vector, y_k can be derived using equation (2.12). The KPCA-based feature approach selects the primary components from a walking image sequence, forming a biometric feature vector to represent a given participant. The sequential gait image frames and the associated sequential primary KPCA components (^{1st}KPC) of a non-PD subject are shown in Figures 3.5(a) and 3.5(b).

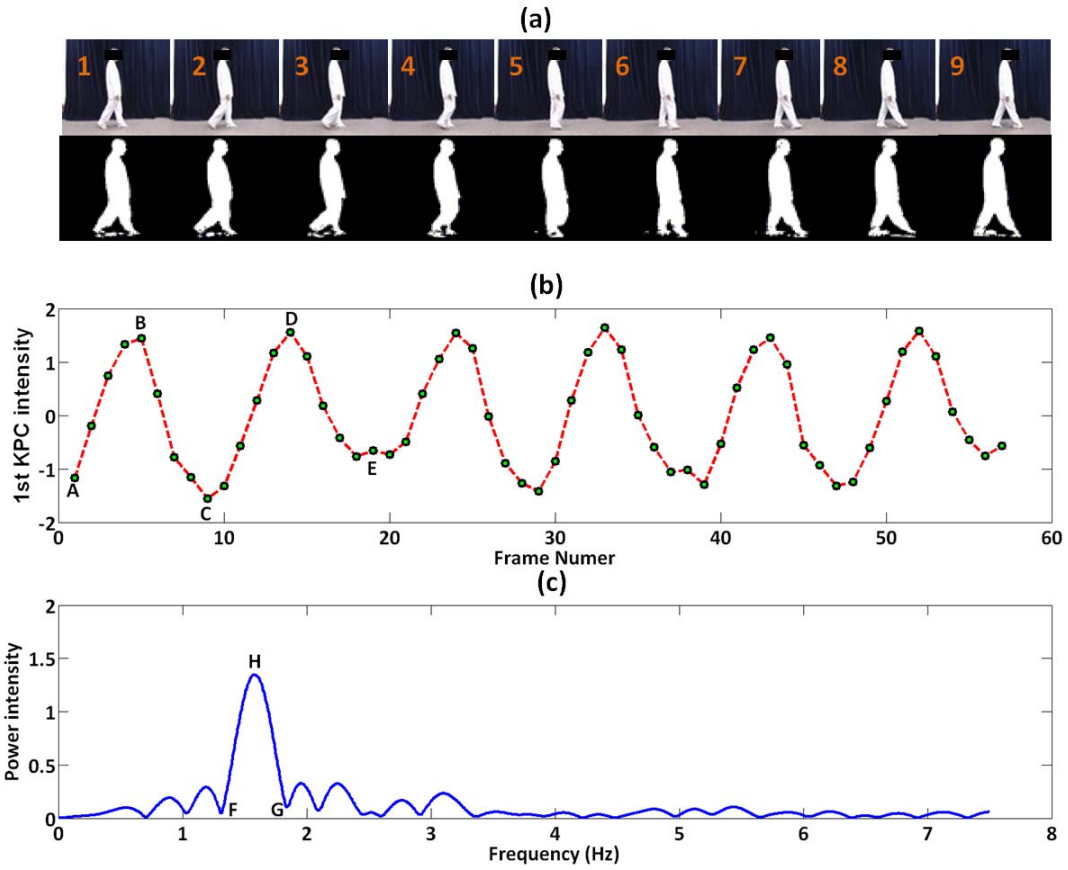

Figure 3.5 (a) Step image frames from a non-PD subject. The top panel is the original sequential walking image frames with 240 × 320 pixels. The bottom panel is the trimmed 64 × 64 pixels binary silhouettes of the top image frames. (b) The magnitudes of the associated sequential primary KPCA components. For simplicity, the primary KPCA component is denoted as ^{1st}KPC. The green dots indicate the magnitudes of the sequential $^{1st}KPCs$. (c) The power spectrum of (b) using a 2048-point DFT and rectangular window with a length, L, of 64 points.

After comparing the gait sequences and associated ^{1st}KPC waveforms, the ^{1st}KPC value (fifth dot, Figure 3.5(b), **B**) reaches a local maximum value when a participant performs a mid-swing event (***frame 5***, Figure 3.5(a)). Moreover, a heel strike event (***frame 1***, Figure 3.5(a)) corresponds to a local minimum ^{1st}KPC value (first dot, Figure 3.5(b), **A**). Similarly, in Figure 3.5(b), the ^{1st}KPC values are at local maximums (fifth and thirteenth dot, Figure 3.5(b), **B** and **D**, respectively) and minimums (first and ninth dot, Figure 3.5(b), **A** and **C**, respectively) at the moment when the non-PD subject is performing mid-stances and heel strikes, respectively.

Using the temporal ^{1st}KPC waveforms, the moment of occurrence of the heel strike can be determined. The distance between two heel strikes can be estimated by the two locations of the heel in the binary 240 × 320 pixels image frames. As a result, the kinematic gait parameters, which depend on the time period and distance between two heel strikes that are performed with the same foot, gait cycle time, stride length, walking velocity and cadence can be estimated. The power spectrum of the temporally associated ^{1st}KPC is plotted in Figure 3.5(c), and the main lobe frequency reflecting the step frequency of the non-PD subject is located at approximately 1.67 Hz.

3.2.6 Minimum Distance Classifier (MDC) for classification

The MDC [69, 70] is a numerical approach used for classify unknown data to classes which minimize the distance between the data and the class in multi-feature space. Because the distance is defined as an index of similarity, the minimum distance is identical to the maximum similarity. In the current study, the efficiency of area, PCA-based, and KPCA-based feature approaches are compared by evaluating their classification sensitivity. An area feature vector is obtained by counting the number of pixels of a particular participant's walking image sequence. On the other hand, the primary PCA and KPCA components per frame are used to form the PCA and KPCA feature vectors for a particular participant, respectively. Gait patterns are classified with a MDC, which is sufficient for the evaluation of feature efficiencies in this study. MDC is used in this study to classify a feature vector y to the to ith class $\boldsymbol{I}$ whose mean $\boldsymbol{m}_i$ has a minimum Euclidian distance to y. The minimum distance classifier can be expressed as

$$\boldsymbol{I} = \arg\min_i \left\{ (\boldsymbol{y} - \mathbf{m}_i)^T (\boldsymbol{y} - \mathbf{m}_i) \right\} \tag{3.5}$$

where $(\mathbf{y}-\mathbf{m}_i)^T(\mathbf{y}-\mathbf{m}_i)$ is the Euclidian distance; *T* is the data of the transposed matrix.

3.2.7 Spectral analyses for temporal gait feature signals

The DFT is a specific method to transform a function in the time domain into the frequency domain for understanding the spectral power distribution of the function [72]. Discrete Fourier Transform (DFT), also called Finite Fourier Transform (FFT), is one of the specific forms of Fourier Transform which has discrete form and finite length in either time domain or frequency domain. It can be recognized as sampling in frequency domain of Discrete Time Fourier Transform (DTFT). For a input function $y[n]$ with $n = 0, 1, \cdots, N-1$, by DFT we can get

$$Y[k] = \sum_{n=0}^{N-1} y[n] e^{-i\frac{2\pi}{N}kn}, \quad k = 1,\ 2,\ \cdots, N-1 \qquad (3.6)$$

The complex numbers $Y[k]$ represents the amplitude and phase of the different sinusoidal components of the input signal $y[n]$. Formally, the transformed series in frequency is periodic and the frequency spectrum can be expressed in a finite duration.

For the spectral gait analyses, ^{1st}KPC is transformed with DFT. The main lobe frequency (corresponding to **H** in Figure 3.5(c)) of the ^{1st}KPC spectrum, representing the gait parameter of the step frequency for a participant, is then computed. Afterwards, the sums of the power within the main lobe between **F** and **G** in Figure 3.5(c) is calculated. The sums of the powers within the main lobe are denoted as $E_{M,N}$, $E_{M,OFF}$ and $E_{M,ON}$ for a non-PD subject, a patient with mild PD in the "Drug-Off" and "Drug-On" states, respectively. The low- and high-frequency counterparts for a participant, denoted as $E_{L,N}$, $E_{L,OFF}$ and $E_{L,ON}$ and $E_{H,N}$, $E_{H,OFF}$ and $E_{H,ON}$, respectively, are also

similarly calculated.

The study was designed to identify the gaits and quantify the gait parameters of the non-PD subjects and the patients with mild PD in the "Drug-On" (proper L-dopa treatment received one hour later) and "Drug-Off" (at least 12 hours after the withdrawal of L-dopa) states. A paired *t*-test was used to examine the differences among the non-PD, "Drug-Off" and "Drug-On" groups. To examine whether the BMI and age make impacts on recognizing the non-PD subject and "Drug-Off" gaits, an analysis of covariance (ANCOVA) test for measurements with covariates BMI and age was applied to evaluate the differences in gait parameters between the two groups. A value of *p* less than 0.05 is considered to be statistically significant. A least significant differences LSD *post hoc* test is performed.

3.2.8 Correlations between the extracted gait parameters and the five sub-scores in the part III of UPDRS

The extracted gait parameters of gait cycle time, stride length, walking velocity, cadence stride frequencies from the KPCA-based feature in temporal and frequency domains are correlated with the five sub-scores in part III of UPDRS. The correlation coefficient between the observation assessment and the image-based gait analysis is investigated with the Pearson product-moment correlation, shown as

$$r = \frac{1}{N-1}\sum_{i=1}^{N}\left(\frac{x_i-\bar{x}}{s_x}\right)\left(\frac{y_i-\bar{y}}{s_y}\right) \tag{3.7}$$

where x and y are two datasets of variable of interest, x_i and y_i are the ith data points of x

and y respectively, $\bar{x}$ and $\bar{y}$ are the sample means of datasets x and y, s_x and s_y are the sample standard deviation (S.D.) of x and y, N is the amount of data points of dataset, and r is the correlation coefficient. If the p-value < 0.05, which means our method has the expected and equivalent capability close to the five subscores in UPDRS part III and may describe the motor impairment.

3.3 Results

3.3.1 Five UPDRS part III subscores of the patients with mild PD in the "Drug Off" and "Drug On" states

Five subscores—axial score (summation of UPDRS part III items 18, 22 with neck only, 27, 28, 29, and 30), limb akinesia (summation of items 23, 24, 25, and 26), limb rigidity (item 22 with neck excluded), limb tremor (summation of items 20 and 21), and part III (summation of items 18 to 31)—are computed according to the UPDRS part III motor scores (table 3.2) to describe the motor deviation of the patients with mild PD in different states (table 3.3). After the L-dopa treatment, the five subscores of all the patients with mild PD are improved; 10 patients with mild PD show an increase of less than 20 points on the Part III scores.

Table 3.2 UPDRS part III motor scores during the"Drug-Off" and"Drug-On" states.

Patient	1	2	3	4	5	6	7	8	9	10	11	12
Drug	Off/On	Off/On	Off/On	Off/On	Off/On	Off/On	Off/On	Off/On	Off/On	Off/On	Off/On	Off/On
18 .speech	2/2	1/1	2/2	0/0	1/1	0/0	1/1	1/1	1/0	1/1	1/1	1/1
19. Facial expression	1/1	0/0	2/2	1/1	1/0	0/0	2/1	1/1	2/1	1/1	1/1	1/1
20. Tremor at rest												
Face	0/0	0/0	0/0	0/0	0/0	0/0	0/0	0/0	0/0	0/0	0/0	0/0
Hand R,L	1,0/1,0	3,1/1,0	0,3/0,3	2,1/2,0	0,0/0,0	1,0/1,0	1,1/0,0	2,0/0,0	0,1/0,0	0,3/0,3	0,0/0,0	0,0/0,0
Feet R,L	1,2/0,0	1,0/0,0	2,0/1,1	1,0/0,0	0,0/0,0	0,0/0,0	0,0/0,0	2,0/0,0	1,0/0,0	1,2/1,2	0,0/0,0	0,0/0,0
21. Action tremor R,L	0,0/0,0	2,1/1,0	0,0/0,0	1,1/0,0	0,0/0,0	1,0/1,0	1,1/1,1	1,1/0,0	2,2/0,0	0,3/0,2	0,0/0,0	0,0/0,0
22. Rigidity												
Neck	2/1	2/2	2/2	2/2	0/0	0/0	2/1	2/1	2/0	1/0	1/1	2/2
UE R,L	2,1/1,0	3,2/2,1	2,3/1,2	2,2/2,1	1,2/0,2	3,2/2,1	3,2/2,1	1,2/0,1	1,2/0,0	0,2/0,1	1,3/0,2	2,2/2,2
LE R,L	2,1/1,1	2,2/2,1	3,3/2,3	2,3/1,2	0,1/0,1	1,0/0,0	2,2/1,1	2,2/0,1	3,2/2,1	0,1/0,0	1,2/1,2	2,1/2,1
23. Finger taps R,L	0,2/0,0	2,1/1,1	2,2/1,2	1,1/0,1	1,2/1,1	1,1/1,0	2,3/1,1	2,2/1,1	1,2/1,2	0,3/0,2	1,2/1,1	1,2/1,2
24. Hand grips R,L	0,1/0,0	2,1/1,1	1,2/1,2	2,1/1,1	0,1/0,1	1,1/1,1	2,2/1,1	2,1/1,1	2,2/1,2	0,2/0,2	1,3/1,2	1,1/1,1
25. RAMH R,L	0,2/0,2	3,1/1,0	2,3/1,3	2,2/2,2	1,2/0,0	1,0/1,0	2,2/1,1	2,2/2,2	1,2/1,1	0,3/0,2	1,3/1,3	1,2/1,1
26. Leg agility R,L	2,2/0,0	2,1/1,0	3,3/3,3	1,1/0,1	0,1/0,1	1,0/0,0	1,1/0,0	1,1/0,0	2,2/0,0	0,1/0,1	1,2/1,1	0,0/0,0
27. Arise from chair	3/0	2/1	2/1	1/0	0/0	1/0	1/0	1/1	1/0	0/0	1/1	0/0
28. Posture	1/1	1/1	1/1	1/1	1/1	1/1	3/2	2/2	1/1	0/0	1/1	0/0
29. Gait	1/0	1/1	2/2	1/0	1/0	1/0	1/1	2/1	2/0	1/1	1/1	0/0
30. Postural stability	2/2	0/0	1/1	2/2	1/1	1/1	2/1	2/2	2/1	1/1	1/1	0/0
31 .Body bradykinesia	2/1	2/1	2/2	1/1	1/0	1/1	2/0	2/1	2/1	2/2	2/2	1/1
Part III: total	33/14	39/21	48/42	35/23	18/10	19/12	42/20	39/20	41/14	28/22	30/25	20/19

R: right; L: left; UE: upper extremity; LE: lower extremity; RAMH: rapid alternating movements of hands.

Table 3.3 Definition of the five subscores in the UPDRS part III.

Subscores	**UPDRS part III motor items**
Axial score	18, 22 (neck only), 27, 28, 29, 30
Limb akinesia	23, 24, 25, 26
Limb rigidity	22(without neck)
Limb Tremor	20, 21
Part Ⅲ	18 - 31

3.3.2 Comparison of the sensitivities of the approaches

Classification accuracies using MDC based on the area feature, PCA-based and KPCA-based features to identify different gaits are presented by confusion matrices in table 3.4.

Table 3.4 The confusion matrices use the area feature, PCA and KPCA approaches to classify different gaits.

	Area feature			**PCA**			**KPCA**		
	Non-PD	Drug-Off	Drug-On	Non-PD	Drug-Off	Drug-On	Non-PD	Drug-Off	Drug-On
Non-PD	9	0	3	10	1	1	10	0	2
Drug-Off	1	8	3	2	7	3	2	10	0
Drug-On	6	5	1	3	1	8	2	1	9
Predicted(positive)/ actual(all)	9/12	8/12	1/12	10/12	7/12	8/12	10/12	10/12	9/12
sensitivity	75%	66.67%	8.33%	83.33%	58.33%	66.67%	83.33%	83.33%	75%
Average sensitivity	50.16%			69.44%			80.51%		

In identifying the non-PD subjects from the patients with mild PD in the “Drug-Off” and “Drug-On” states, the separation capabilities of area, PCA-based and KPCA-based features are similar. However, area feature is inadequate in identifying patients with mild PD in the “Drug-On” state. Only one of them is classified correctly, whereas the others are mis-classified as non-PD subjects or patients with mild PD in the “Drug-Off” state. On the other hand, results from the KPCA-based feature approach provide an average sensitivity of 80.51%.

3.3.3 Kinematic gait parameters among different groups

The KPCA-based method was used to extract the gait parameters from the sequential gait video frames from the non-PD subjects, the patients with mild PD in the “Drug-On” and “Drug-Off”

states. The average gait cycle times (s), stride lengths (cm), walking velocities (cm/s), and cadences (steps/min) of these groups are presented in Table 3.5.

Table 3.5 Kinematic and spectral gait parameters (Mean±SD).

	Non-PD (n=12)	*Drug-Off (n=12)*	*Drug-On (n=12)*	*BMI*	*Age*
Gait cycle time (s)	1.21±0.08	*1.16*±0.15	*1.15*±0.12	N.S	N.S
Stride length (cm)	105.48±6.95	*85.54*±17.21	$^{\xi}$*105.94*±22.90	N.S	N.S
Walking velocity (cm/s)	87.35±8.45	*76.35*±22.84	*93.68*±23.35	N.S	N.S
Cadence (steps/min)	99.33±6.04	*106.45*±15.09	105.88±12.33	N.S	N.S
Step frequency (Hz)	1.66±0.11	*1.48*±0.34	$^{\xi}$*1.74*±0.18	N.S	N.S
EL (%)	9.55±7.84	*16.21*±9.60	$^{\xi}$*9.40*±4.56	N.S	N.S
EM (%)	*75.07±9.36	*63.89*±11.63	72.58±8.63	N.S	N.S
EH (%)	15.37±3.10	*19.88*±8.25	*18.00*±6.31	N.S	N.S

$^{*, \xi}$ are significant ($p < 0.05$) regarding the non-PD subject and patients with mild PD in the "Drug-Off" state, and the patients with mild PD in the "Drug-Off" and "Drug-On" states. EL, EM, and EH are the percent of energy distributed in the low-frequency band, main-frequency band, and high-frequency band, respectively. Interactions between *factors* (BMI and AGE) and *Groups* (Non-PD and Drug-Off) were assessed by ANCOVA. N.S is non-significant ($p > 0.05$).

The patients with mild PD showed improvements in all gait parameters after receiving L-dopa, but only stride length showed significant improvement. Compared to the patients with mild PD in the "Drug-Off" state, the non-PD subjects manifested better gait performance in terms of stride length and walking velocity, but their performance was worse than the patients with mild PD in the "Drug-On" state across all kinematic gait parameters. Moreover, the non-PD subjects showed no significant differences in the kinematic gait parameters compared to the patients with mild PD in the "Drug-Off" and "Drug-On" states. ANCOVA measurements were used to analyze the interaction between factors (BMI and age) and groups (Non-PD and Drug-Off). We find found that there were no significant differences in the interactions between the factors and groups.

Figure 3.6 presents examples of the ^{1st}*KPC* waveforms from a non-PD subject, a patient with mild PD in the "Drug-Off" and "Drug-On" states. The ^{1st}*KPC* waveforms of the patient with mild PD in the "Drug-On" state were similar to those of the non-PD subject, whereas the waveforms of patients with mild PD in the "Drug-Off" state tended to be rather irregular.

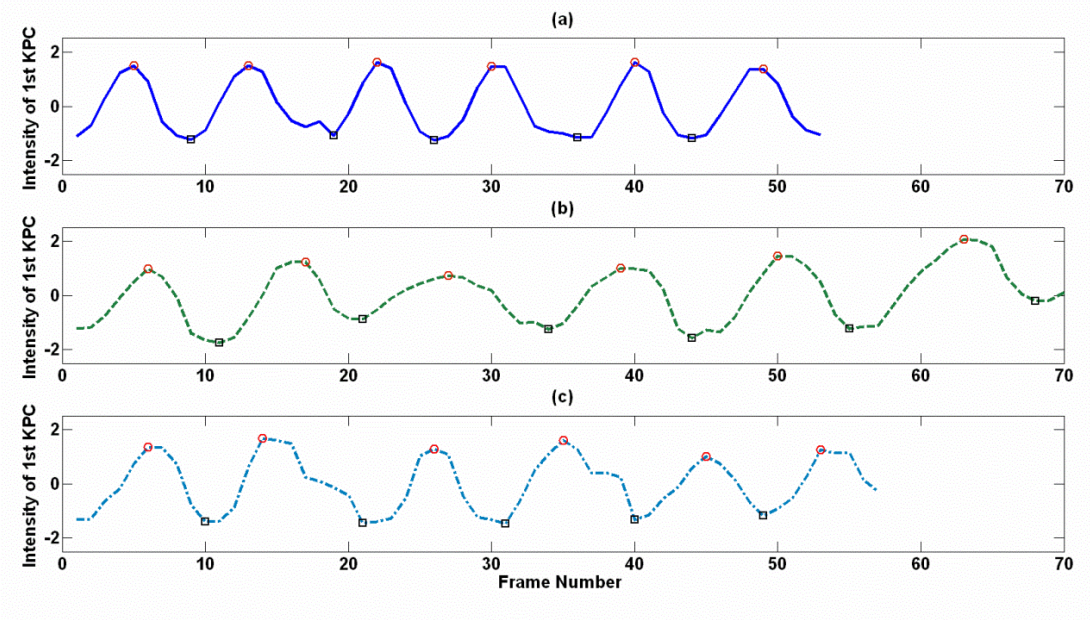

Figure 3.6 (a) The *1st KPC* waveform of a selected non-PD subject. (b) The *1st KPC* waveform of a selected patient with mild PD in the "Drug-Off" state. (c) The 1stKPC waveform of the same patient with mild PD in the "Drug-On" state. The red circles and black squares represent the local maximums and minimums, which reflect the occurrences of mid-swings and heel strikes, respectively.

3.3.4 Power spectrum of temporal gait signals

The gait frequency spectra of the patients with mild PD in the "Drug-Off/On" states and the non-PD subjects are shown in Figure 3.7. The average step frequencies of the non-PD subjects and patients with mild PD in the "Drug-On" and "Drug-Off" states are 1.661, 1.743 and 1.543 Hz, respectively. The comparisons of the step frequency and spectrum power distributions among the three groups are shown in table 3.5. The results from a paired *t*-test indicate that patients with mild PD in the "Drug-On" state show significant improvement in step frequency. Moreover, $E_{M,NON}$ is significantly larger than $E_{M,OFF}$, and $E_{L,ON}$ is significantly larger than $E_{L,OFF}$.

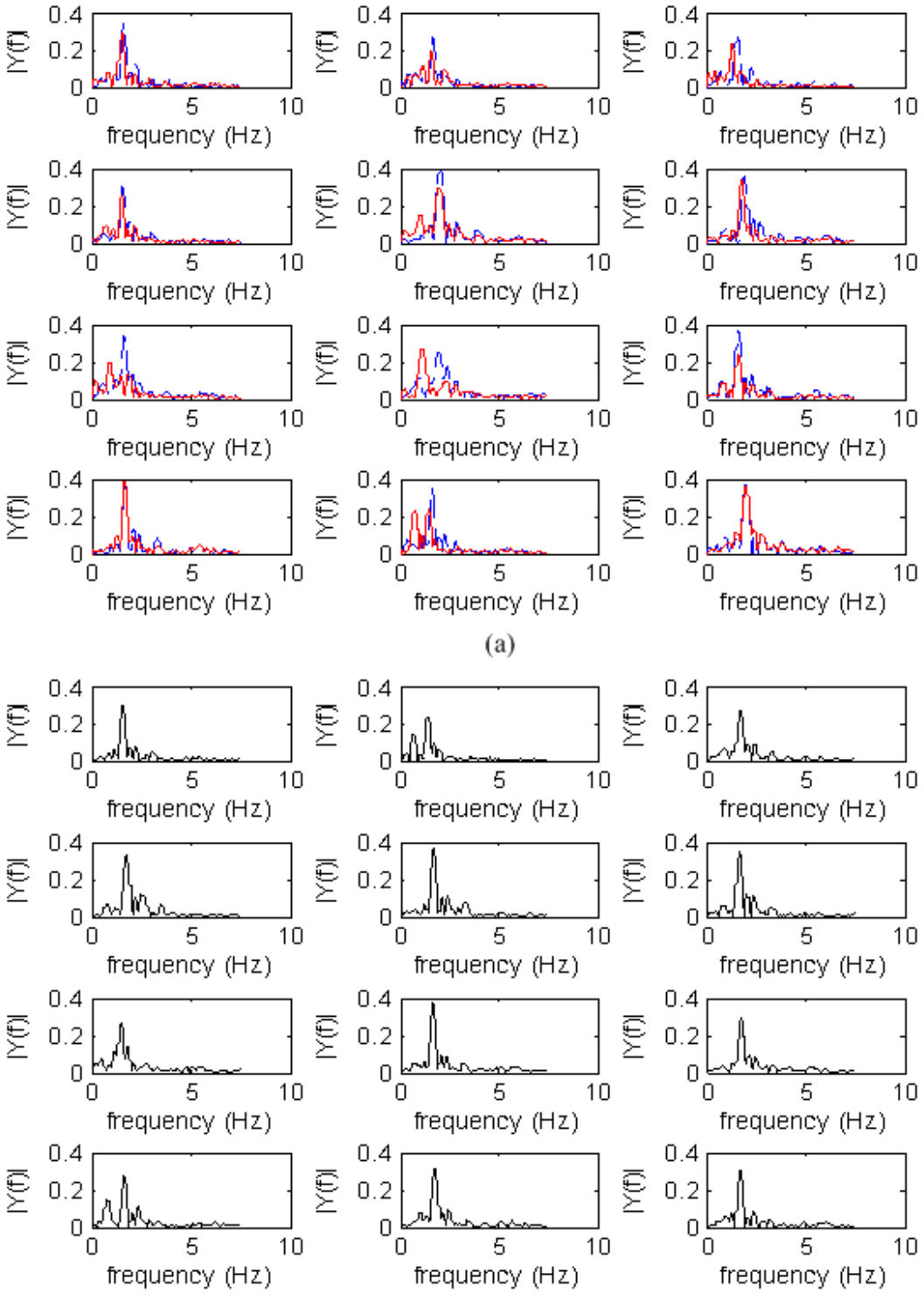

Figure 3.7 The gait frequency spectra of (a) patients with mild PD in the “Drug-Off” state (red solid line) and the “Drug-On” state and (b) the non-PD subjects.

3.3.5 Correlations between the gait parameters and five UPDRS part III subscores

The correlation coefficients between the gait parameters extracted using the KPCA features and the five UPDRS part III subscores are presented in Table 3.6. It is shown that all gait parameters, except cadence, are significantly correlated to at least 3 subscores.

Table 3.6. Correlation coefficients between the five subscores and the extracted gait parameters.

	Axial score	Limb akinesia	Limb rigidity	Limb tremor	Part III
Gait cycle time	N.S.	0.470	0.462	N.S.	0.483
Stride length	0.731	0.479	0.543	N.S.	0.625
Walking velocity	0.686	0.538	0.559	0.413	0.661
Cadence	N.S.	N.S.	N.S.	N.S.	N.S.
Stride frequency	0.693	0.667	0.558	0.438	0.742

N.S. indicates “not significant”

3.4 Discussions

3.4.1 The sensitivity of the KPCA-based gait recognition method

As parkinsonian gait is commonly accompanied by not only slowness in walking and shuffling steps, but also a reduction in hand swing and a stooped posture; thus, information regarding upper extremities and trunk movements facilitate the identification of patients with mild PD [4, 51]. The silhouette approach proposed in this study aims to develop a parkinsonian gait recognition method. Two parkinsonian gait recognition algorithms, the KPCA-based and PCA-based, as well as the area feature approaches, were tested for their abilities to classify the gait of the “non-PD” subjects and the patients with mild PD in different states. The area feature approach is worst at identifying the patients with mild PD in the “Drug-On” state. Only one out of 12 patients with mild PD in the “Drug-On” state is correctly identified and classified; the rest are incorrectly identified as non-PD subjects or patients with mild PD in the “Drug-Off” state. The area feature approach calculates the area occupied by an object (in this case, a participant) in an image frame (i.e., the number of pixels), which may be similar under different conditions. Thus, the poor sensitivity of the area feature

approach is not surprising. The average sensitivity of the PCA-based feature approach is 69.44%, which is better than the area feature method. Nonetheless, the average sensitivity of the KPCA-based feature approach is the highest at 80.51%. Such results are expected; although PCA is appropriate in decomposing images with linear components, the spatiotemporal characteristics associated with abnormalities in gait and upper extremity and trunk movements contain nonlinear principal components.

3.4.2 Gait parameter analysis

Quantitative gait performance is an important reference for early detection and diagnosis of PD and the improvement brought about by scheduled medical treatments. Our results show that the patients with mild PD who receive the L-dopa treatment show improvement in their gait cycle time, stride length, walking velocity, cadence, and step frequency. Such results are consistent with the findings in prior studies [73-75]. However, the patients with mild PD show significant improvements in only their stride length and step frequency in the "Drug-On" state. The improvements in gait cycle time, cadence, and walking velocity are not significant, whereas reductions in gait irregularity and motor symptoms were observed. The results show that the improvements in PD gait are not robust. Nevertheless, the proposed method presented a promising sensitivity in identifying the patients with mild PD in the "Drug-Off" and "Drug-On" states.

Besides, the PD patients in this study are in the mild stages of the disease and present no significant deficits or deterioration in motor functions, they move normally or with only a slight impairment after receiving L-dopa. In this study, the non-PD subjects recruited were healthy adults of nearly the same age and the similar BMI as the patients with mild PD. Given that the healthy and patient groups had similar physical conditions, there were no significant differences in gait performance between the two groups. As the patients with mild PD in the "Drug-On" state presented the nearly the same gait performance as the non-PD subjects, it becomes a big difficulty

to identify two groups. As shown in Figure 3.6 (a) and (b), the ^{1st}KPC waveforms from walking cycles performed by a "non-PD" subject and a patient with mild PD during the "Drug On" state are similar, suggesting the difficulty in identifying the mild parkinsonian gait with inspection using eyes. However, the proposed method once again showed a promising sensitivity in identifying the non-PD subjects and the patients with mild PD in the "Drug-On" state.

In Figure 3.6(c), a longer gait cycle time and the freezing of gait and slowness in motion resulted from body bradykinesia can be identified from the irregular and gentle parts. Due to the slow and asymmetry and unstable walking of the patients with mild PD during the "Drug-Off" state, the ^{1st}KPC waveforms appear to be irregular and different from the non-PD subject's ^{1st}KPC waveform. In fact, the slowness in the walking cycle shifts the main frequency of the ^{1st}KPC waveform toward a lower frequency band. Compared with the patients with mild PD during the "Drug-On" state, approximately 8% of the energy is shifted from the main frequency (Drug On: 73.86%, Drug Off: 66.10%) to a lower frequency band (Drug On: 8.34%, Drug Off: 16.95%) for the patients with mild PD in the "Drug-Off" state. The change in the power distribution causes the temporal ^{1st}KPC waveform, resulting in a failure to form regular waveforms resembling those of non-PD subjects. Such results show that the lack of dopamine in the basal ganglia circuit in the brain may cause abnormalities and irregularities in the gait profile.

3.4.3 Correlations between the five UPDRS III subscores and the extracted gait parameters

The correlations between the extracted gait parameters and the five UPDRS part III subscores are calculated and all gait parameters are significantly correlated to at least three subscores, with the exception of cadence. It is worthwhile to note that limb akinesia, limb rigidity and limb tremor show significant correlations with some gait parameters, despite the lack of items used to evaluate

gait or posture. The findings are consistent with the results described in [76]; thus, it is possible for the therapists to evaluate the motor function of upper extremities of patients with mild PD through gait parameters. The results also support the findings in [77], which describes how the deterioration in upper extremity motor functions contributes to the identification of parkinsonian gait.

In addition, the proposed approach provides the power spectrums of the participant's gait as additional information to analyze the irregularity of the motions of patients with mild PD.

3.5 Conclusion

The abilities to recognize the mild parkinsonian gait and monitor the disease's progression are important clinical issues. However, previous research has been hindered due to the lack of a reliable tool that can be easily installed, provide prompt gait analysis, facilitate data collection and gait analysis, and lower a patient's level of exertion during the examinations. In this study, a computer vision-based gait analysis approach that uses kernel-based principal component analysis is developed. It only requires a digital camera and a decorated corridor to facilitate the classification and quantification of specific gait patterns. Although there is a high similarity in the gait patterns between the patients with mild PD and non-PD subjects, the proposed method presents an encouraging classification sensitivity of 80.51%. Besides, the quantification of the mild parkinsonian gait can also be easy obtained and therefore the clinicians may evaluate the improvement brought about by scheduled medical treatments and monitor the progression of this disease. The significant correlations between the gait parameters and five UPDRS part III subscores

are also acquired and suggest that the gait parameters may also facilitate the assessment of motor deviations of patients with mild PD.

Chapter 4 Quantitative analysis of parkinsoian gait initiation and symmetry using centroid tracking algorithm

4.1 Background and motivations

Hypthesis 2: The gait initiation and symmetry are deteriorated in the early stages of Parkinson's disease. Thus, it is possible to identify the parkinsonian gait from the monocular image sequences using a method that analyzes the gait performance and symmetry during the gait initiation period.

In the previous chapter, we have introduced a KPCA-based method using monocular video image sequences to carry out the recognition and quantification of parkinsonian gait. The ease of use and installation of the previous proposed method provides clinicians and researchers a low cost solution to monitor the progression of and the treatment to PD. However, the demand for space was not well-addressed in the 1st part of this study due to an approximately 6-m decorated corridor required.

Disorder gait initiation [6, 52, 53] and walking symmetry [54, 55, 57] are cardinal symptoms and are commonly used to monitor the progression of PD and estimate the postural instability of PD patients in the early stages. As the evaluation of gait initiation requires a relative small space and is much easier to carry out at clinics with spacious limitation, we are prompted to develop a 2nd method that recognizes the mild parkinsonian gait using the quantitative analysis of parkinsonian gait initiation and symmetry.

In this chapter, the centroid tracking algorithm (CTA) for object tracking is developed to enhance the proposed method in obtaining quantitative gait parameters and associated symmetry indexes during the gait initiation and steady-state walking periods for aiding clinicians to recognize the patients with mild PD, evaluate the improvement brought about by the levodopa, and monitor the progression of PD.

4.2 Methods

4.2.1 The participants

A total of 10 patients with mild PD (8 males and 2 females) with an average age of 59.6 years old (max = 68, min = 44, standard deviation [S.D.] = 6.78), an average weight of 67 kg (max = 76.5, min = 46, S.D. = 9.7), and an average L-dopa dose per treatment of 243.7 mg (max = 375, min = 125, S.D. = 68.8) are recruited as a PD group from Buddhist Tzu Chi General Hospital, Hualien, Taiwan. Another 10 neurologically intact participants (6 males and 4 females) with an average age of 54.4 years old (max = 67, min = 48, S.D. = 5.8) and an average weight of 62.2 kg (max = 75.5, min = 51, S.D. = 9) are recruited into a non-PD group. All participants are giving informed written consent prior to participation.

The patients with mild PD given L-dopa at an equivalent daily dose (LEDD) for one hour were classified as “Drug-On”, whereas those that abstained from L-dopa treatment for at least 12 hours were classified as “Drug-Off”. The patients with mild PD were asked to abstain from L-dopa overnight for at least 12 hours prior to the gait measurements. They then performed drug-off trials

in the morning. Immediately following the completion of the drug-off trials, they were given L-dopa at an equivalent daily dose. Drug-on trials were then assessed one hour after L-dopa given.

All patients with mild PD are physically independent. One patient was reported as having mild unilateral motor symptoms with axial involvement on his left side. Nine patients had mild bilateral motor symptoms disease, with recovery on pull test. Six of nine patients were predominantly diseased on their left sides. Three of nine patients were predominantly diseased on their right sides.

In the "Drug-Off" state, the patients with mild PD scored an average rating 2.45 on the Hoehn & Yahr (H&Y) scale [78] (max = 3, min = 1.5, S.D. = 0.5); whereas the average rating was 2.35 (max = 3, min = 1.5, S.D. = 0.4) in the "Drug-On" state. The clinical performances of all patients with mild PD both states are also estimated using part III of unified Parkinson's disease rating scale (UPDRS) scores [67]. The patients with mild PD in the "Drug-On" state showed an average reduction of 7.8 on UPDRS part III score (max = 21, min = 2. S.D. = 6.8). The characteristics of the participants in both groups are presented in Table 4.1.

Table 4.1 The characteristics of patients with mild PD and non-PD subjects in this study

	patients with mild PD								non-PD subjects		
					H&Y stage		UPDRS III total score				
Subject	Age	Sex	Weight(kg)	L-dopa (mg)	Drug-Off	Drug-On	Drug-Off	Drug-On	Age	Sex	Weight(kg)
1	44	M	73.5	125	1.5	1.5	10	8	52	M	52
2	61	F	74.7	375	3	2.5	44	26	50	M	71
3	67	M	71	187.5	2	2	46	35	57	M	54
4	65	M	72	250	2.5	2.5	25	23	48	M	72.5
5	57	M	61	250	3	3	52	49	67	F	56
6	59	M	71	187.5	2	2	21	16	57	F	65
7	57	M	56	250	2.5	2.5	28	24	48	F	51
8	68	M	68	250	2.5	2.5	26	18	51	F	60
9	59	F	46	312.5	3	2.5	47	26	57	M	65
10	59	M	76.5	250	2.5	2.5	13	9	57	M	75.5

The H&Y stage and UPDRS III total score refer to the “Drug-Off” and “Drug-On” states.

4.2.2 Environmental setup and video recording standard

The environmental setup is shown in Figure 4.1(a). A video camera (VPC-HD1010, Sanyo Corp., Ltd, Japan) is stationed approximately 4.5 m away from the pathway, perpendicular to the participants’ walking direction. Participants are asked to walk barefoot along a 4-m pathway at their pace to naturally reflect their gait performance after receiving a vocal instruction. Each participant is asked to perform four left-to-right walking trials, starting with the right leg, as well as four right-to-left walking trials, starting with the left leg, for a total of eight successful trials. Between trials, the participants were instructed to rest for at least five minutes until their strength was recovered.

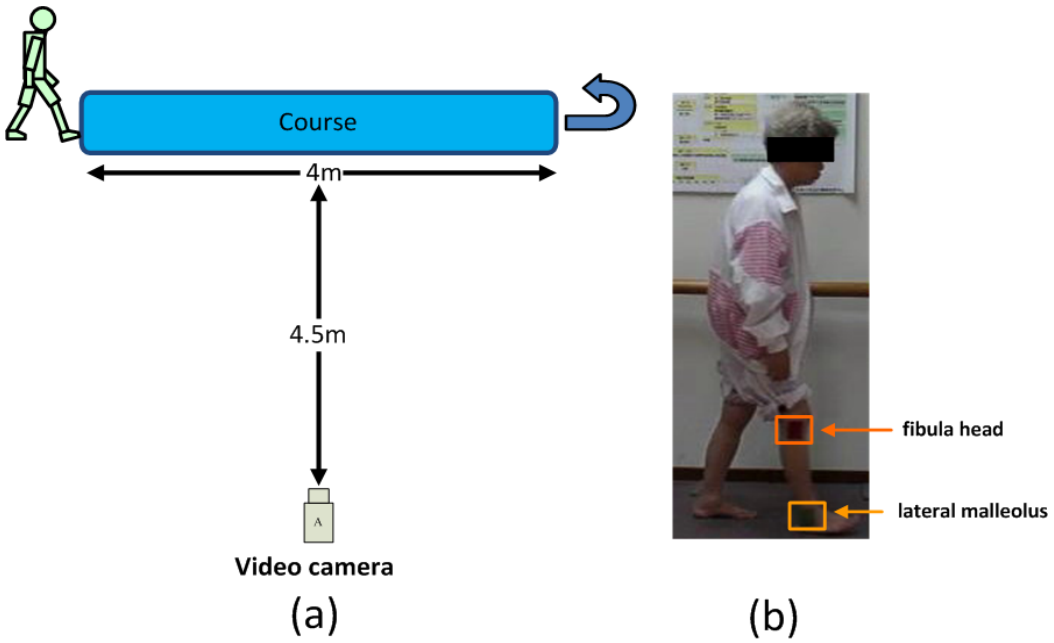

Figure 4.1 (a) The environmental setup includes a camera at a distance of 4.5-m from the front end of the pathway and a 4-m pathway of participants' walking direction. (b) The position of markers on a participant's the fibula head and lateral malleolus.

Referring to a prior study [31], gait initiation and steady-state walking periods are defined as the duration beginning from the vocal instruction for gait initiation to heel strike of the first swing leg in a gait sequence, and the duration starts from toe off of the first stance leg to the final heel strike in a gait sequence walking states, respectively. The descriptive stages during the gait initiation and steady-state walking periods are presented in Figure 4.2. The first step length is defined as the distance between heels of the first stance leg and the first swing leg at the moment when the first swing leg contacted the ground, indicating the proceeding distance during the gait initiation period.

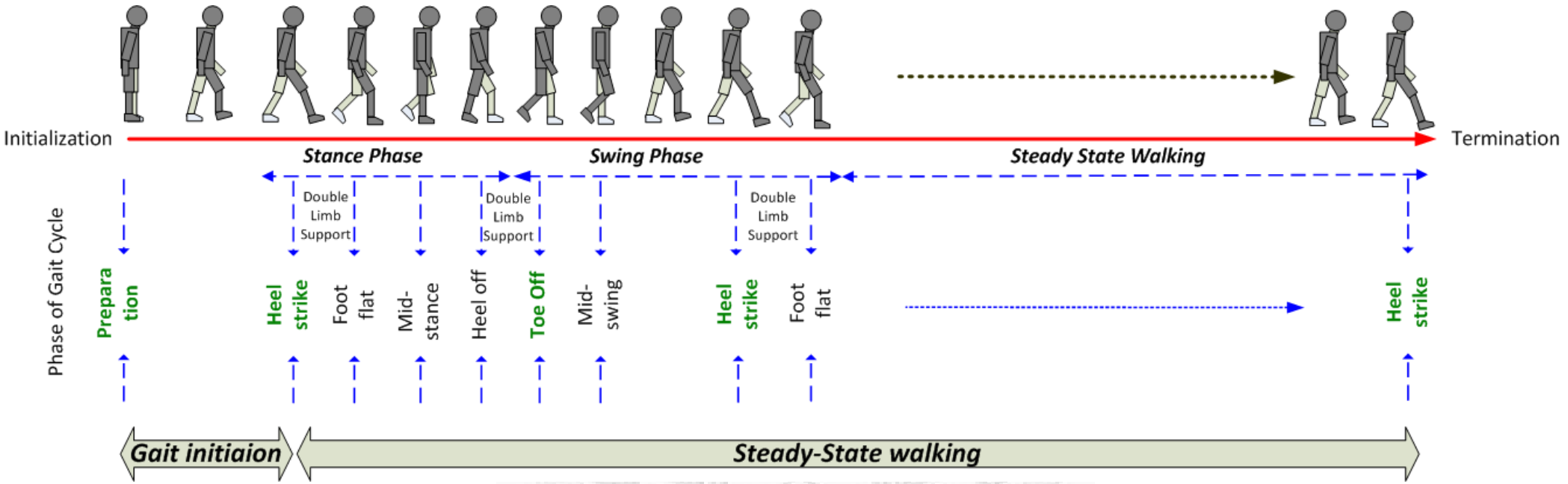

Figure 4.2 Descriptive stages during the gait initiation and steady-state walking periods.

All captured walking dynamic data was sent to a host computer and clipped automatically with a sampling rate of 60 frames/sec. The resolution of each image is 640 × 480 pixels, with an image spatial resolution of 1.6 pixels/cm. As the video camera was not equipped with an excitation filter, the reflective markers cannot be detected. In addition, the image spatial resolution was too low to accurately identify the conventional small and spherical markers. Therefore, as shown in Figure 4.1(b), two 5 × 5 cm square color tapes were used as tracking tags to mark the positions of the fibula head and lateral malleolus during all trials. They were attached to two anatomic bony landmarks, the fibula head and the lateral malleolus of the leg. Thereafter, the proposed camera-based gait tracking and analysis system, implemented with MATLAB R11 (Mathworks Inc., USA), was conducted for further signal processing.

4.2.3 The centroid tracking algorithm to determine the heel strike and toe off events

Heel strike and toe off events are necessary for reconstructing the gait pattern and quantifying gait parameters and further statistical analysis. In this study, the derivative of shank angle variation, the shank angular velocity, is used to determine the heel strike and toe off events during each gait sequence. Traditional methods record the moving trajectories of tags on hip, knee, and ankle and then compute the shank variation angle θ (in degrees) during walking (as shown in Figure 4.3(a)). However, in this study, the determination of the shank angular velocity is different. The acquirement of shank angle variation uses two tracking tags attached on the fibula head and lateral malleolus to compute the variation angle $\hat{\theta}$ (in degrees) during walking (as shown in Figure

4.3(b)). A red solid line (a plumb line) perpendicular to the ground from the tracking tag on the fibula head is traced in each image frame. It is treated as a zero degree ($\hat{\theta}=0^{o}$) reference for calibration in image post-processing. Noted that hip flexion is not required for the determination of shank angle variation angle.

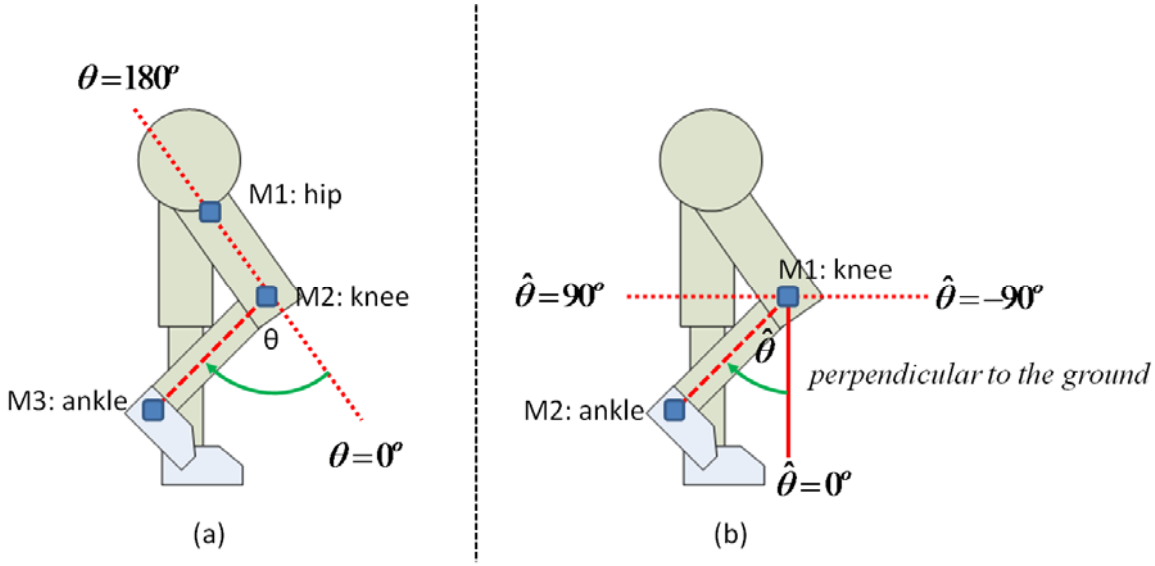

Figure 4.3 The representation of how the proposed method uses two joint identifiers to calculate the shank angle variation. (a) The traditional method using three joint markers secured on hip, knee, and ankle joints. (b) The proposed method using two joint markers secured on knee and ankle joints, respectively. The red solid line is a plumb line and treated as a zero degree reference for calibration in image post-processing. The red dotted line is a line horizontal to the ground. The angle between the red solid and red dashed lines is the shank angle variation derived.

In the present study, the CTA introduced in chapter 2 is used to detect the moving trajectories of the two tags, by which the knee and ankle joint movements during trials are recorded. Using the CTA, the shank angle variation during walking can be computed conveniently. According to a previous study [79], the heel strike and toe off events can be effortlessly determined through shank angular velocity.

The quantitative gait parameters during the gait initiation and steady-state walking periods both can be derived once the heel strike and toe off events are determined. In Figure 4.4, the shank angle

variation in degrees and the associated angular velocity from a mild PD patient's walking trial are shown as the top and bottom illustrations, respectively.

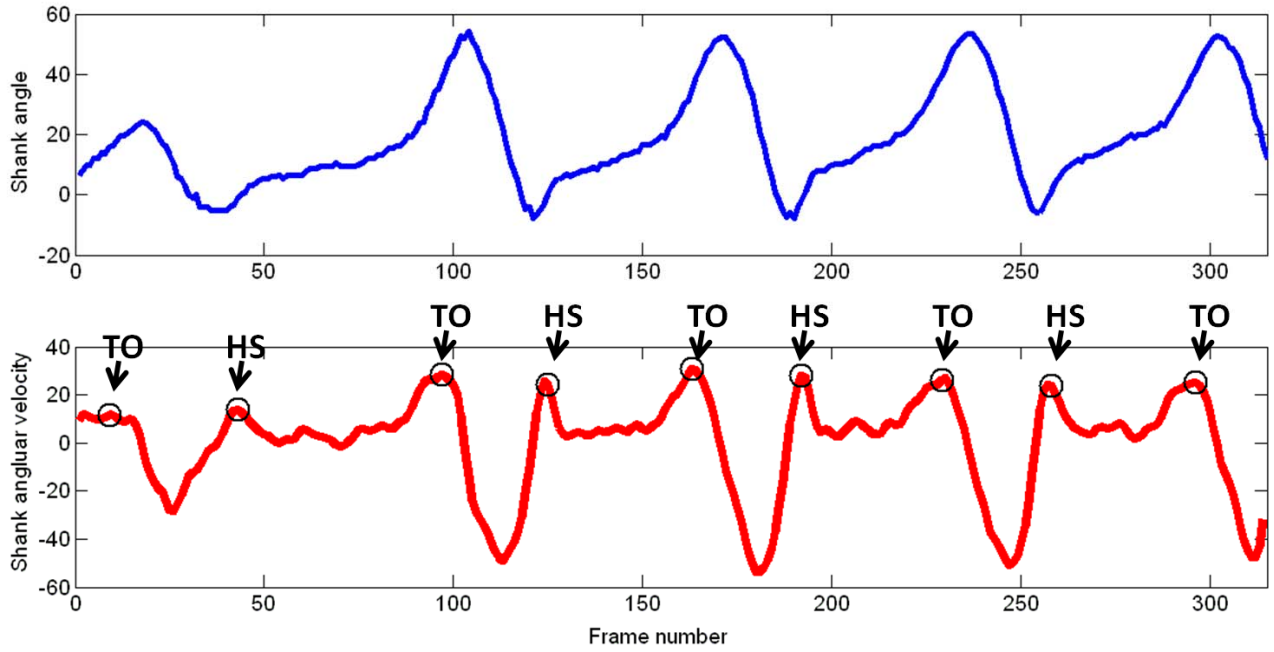

Figure 4.4 The shank angle variation and associated angular velocity in a gait sequence performed by a patient with mild PD. The circles are the moments of the occurrences of heel strike and toe off events. TO and HS are toe off and heel strike events, respectively.

The index of frame reflects time interval equivalent to the inverse of the clipping rate. An example of the variation of a mild PD patient's shank angle is shown in Figure 4.4 and heel strike and toe off events are identified with circles, respectively. After the heel strike and toe off events are determined, the kinematic gait parameters during the gait initiation and steady-state walking periods of each walking sequence can be extracted to examine the differences in gait performance between different states in non-PD subjects and patients with mild PD.

To verify the validity of the video-based gait tracking and analysis system, a commercial gait analysis technique, the Vicon system (Oxford Metrics Group; Oxford, UK), is selected for validity verification. Results indicate that there is no significant difference between the proposed system and

the compared techniques in providing gait parameters, including stance phase (% of gait cycle), walking velocity (cm/sec), and cadence (steps/min) for further gait parameter analysis (please refer to **Appendix C** for details).

4.2.4 Gait symmetry index

Gait symmetry information is another important indication of the severity of the loss of walking balance in people with neuromuscular issues, including PD. Robinson et al. proposed a symmetry index (SI) equation [80], which is reported in [81, 82] and defined below:

$$SI = \frac{|X_R - X_L|}{0.5(X_R + X_L)} \times 100\% \tag{4.4}$$

where X_R and X_L are the values of any gait parameter measured from the right and left lower limbs, respectively. To avoid side (right/left) or paretic/non-paretic limb discrimination, the absolute value is applied for the subtraction item. The magnitude of SI indicates the degree of asymmetry, ranging from 0 to 200%. When SI = 0, the gait is at perfect symmetry; an increase in SI implies an increase in the asymmetry of the gait parameter. Notably, step length, swing time, and swing speed during gait initiation and steady-state walking periods are measured to derive gait symmetry index in different states.

4.2.5 Data statistics

The experiment was designed to quantitatively compare differences in gait parameters and symmetry indexes in non-PD subjects and patients with mild PD. A paired *t*-test is conducted to find the differences in the gait parameters and symmetry indexes between the patients with mild PD

in “Drug-On” and “Drug-Off” states. A two-sample *t*-test is used to compare the differences in gait parameters and symmetry indexes between the non-PD subjects and patients with mild PD. A value of p less than 0.05 is considered to be significant.

4.3 Results

4.3.1 Comparisons of gait parameters and symmetry indexes during the steady-state walking between non-PD subjects and patients with mild PD

The averages of the gait parameters during the steady-state walking for non-PD subjects and patients with mild PD in the “Drug-Off” and “Drug-On” states are shown in Table 4.2.

Table 4.2 Comparisons of the gait parameters and symmetry index during steady state walking period among non-PD subjects and patients with mild PD in different states. All values are presented as mean ± standard deviation.

Gait Parameter	Non-PD	Drug-Off	Drug-On
Gait Cycle Time (sec)	1.13 ± 0.15	1.07 ± 0.08	1.06 ± 0.11
Stance Phase (%GC)	62.20 ± 1.82	62.6 ± 2.65	62.03 ± 1.46
Walking Velocity (cm/sec) %LL	*1.18 ± 0.20	0.94 ± 0.19	$^{\xi}$1.19 ± 0.18
Cadence (steps/min)	107.93 ± 14.34	113.18 ± 8.41	114.84 ± 11.50
Step Length (cm) %LL	*1.09 ± 0.11	0.92 ± 0.19	$^{\xi}$1.08 ± 0.09
Swing Time (sec)	$^{*,\lambda}$0.44 ± 0.05	0.39 ± 0.03	0.39 ± 0.04
Step Speed (cm/sec) %LL	*2.65 ± 0.34	2.20 ± 0.34	$^{\xi}$2.71 ± 0.38
Symmetry Index	Non-PD	Drug-Off	Drug-On
Gait Cycle Time (%)	*1.44 ± 1.23	2.56 ± 1.16	2.06 ± 2.62
Stance Phase (%)	$^{\lambda}$1.21 ± 0.67	3.06 ± 3.06	3.13 ± 2.81
Step Length (%)	$^{*,\lambda}$0.99 ± 0.84	3.36 ± 1.93	2.75 ± 1.49
Swing Time (%)	$^{*,\lambda}$1.19 ± 1.10	6.03 ± 3.80	5.44 ± 4.59
Step Speed (%)	$^{*,\lambda}$0.77 ± 0.78	5.59 ± 3.26	3.52 ± 2.95

% LL is normalized by leg length. %GC is percent of gait cycle.

$^{*, \lambda, \xi}$ represent significant differences ($p < 0.05$) between the non-PD subjects and patients with mild PD in the “Drug-Off” state, non-PD subjects and patients with mild PD in the “Drug-On” state, and patients with mild PD in the “Drug-Off” and “Drug-On” states.

The associated symmetry indexes are also shown in Table 4.2. In the "Drug-Off" state, the mean step length of patients with mild PD is significantly shorter than that of the non-PD subjects (0.92 ± 0.19 vs. 1.09 ± 0.11, $p < 0.05$). The mean swing time of patients with mild PD is significantly shorter than that of the non-PD subjects (0.39 ± 0.03 vs. 0.44 ± 0.05, $p < 0.05$). The mean walking velocity and step speed in patients with mild PD are significantly less than those of the non-PD subjects (0.94 ± 0.19 vs. 1.18 ± 0.20, $p < 0.05$ and 2.20 ± 0.34 vs. 2.65 ± 0.34, $p < 0.01$, respectively). The patients with mild PD in the "Drug-Off" state show a slight but non-significant increase in their cadence and stance phase and reduction in gait cycle time as compared to the non-PD subjects. The symmetry indexes of patients with mild PD in the "Drug-Off" state are significantly greater than those of the non-PD subjects, in terms of gait cycle time (2.56 ± 1.16 vs. 1.44 ± 1.23, $p < 0.05$), step length (3.36 ± 1.93 vs. 0.99 ± 0.84, $p < 0.01$), swing time (6.03 ± 3.80 vs. 1.19 ± 1.10, $p < 0.01$), and step speed (5.59 ± 3.26 vs. 0.77 ± 0.78, $p < 0.01$). However, no significant differences are observed in the stance phase (% of gait cycle).

In the "Drug-On" state, patients with mild PD display significant increases in walking velocity (1.19 ± 0.18 vs. 0.94 ± 0.19, $p < 0.05$, paired *t*-test), step length (1.08 ± 0.09 vs. 0.92 ± 0.19, $p < 0.05$, paired *t*-test), and step speed (2.71 ± 0.38 vs. 2.20 ± 0.34, $p < 0.05$, paired *t*-test), as compared to the patients with mild PD in the "Drug-Off" state. When compared to non-PD subjects, patients with mild PD in the "Drug-On" state show significant differences in swing time (0.39 ± 0.04 vs. 0.44 ± 0.05, $p < 0.05$, paired *t*-test). However, no significant differences are observed in the other

gait parameters. The symmetry indexes of patients with mild PD in the "Drug-On" state are significantly larger than those of non-PD subjects in terms of the stance phase (3.13 ± 2.81 vs. 1.21 ± 0.67, $p < 0.05$), step length (2.75 ± 1.49 vs. 0.99 ± 0.84, $p < 0.01$), swing time (5.44 ± 4.59 vs. 1.19 ± 1.1, $p < 0.05$), and step speed (3.52 ± 2.95 vs. 0.77 ± 0.78, $p < 0.05$). However, there is no significant improvement in the symmetry indexes observed for patients with mild PD in the "Drug-On" state.

4.3.2 Comparisons of gait parameters and symmetry indexes during the gait initiation period between non-PD subjects and patients with mild PD

The averages of the gait parameters of non-PD subjects and patients with mild PD in the "Drug-Off" or "Drug-On" states during the gait initiation period are presented in Table 4.3.

Table 4.3. Comparisons of gait parameters and symmetry index during the gait initiation period among non-PD subjects and patients with mild PD in different states. All values are presented as mean ± standard deviation.

Gait Parameter	Non-PD	Drug-Off	Drug-On
First Step Length (cm) % LL	*0.55 ± 0.06	0.42 ± 0.11	$^{\xi}$0.53 ± 0.07
First Swing Time (Sec)	0.47 ± 0.06	0.47 ± 0.06	0.49 ± 0.08
First Step Speed (cm/sec) %LL	*1.16 ± 0.27	0.90 ± 0.19	1.07 ± 0.29
Symmetry Index	Non-PD	Drug-Off	Drug-On
First Step Length (%)	$^{*,\lambda}$2.98 ± 4.40	16.36 ± 5.19	13.58 ± 8.58
First Swing Time (%)	$^{*,\lambda}$2.24 ± 2.73	10.98 ± 6.93	12.41 ± 9.88
First Step Speed (%)	$^{*,\lambda}$3.81 ± 3.26	12.02 ± 6.92	16.81 ± 10.41

% LL is normalized by leg length.

$^{*, \lambda, \xi}$ represent significant differences ($p < 0.05$) between the non-PD subjects and patients with mild PD in the "Drug-Off" state, non-PD subjects and patients with mild PD in the "Drug-On" state, and patients with mild PD in the "Drug-Off" and "Drug-On" states.

The associated symmetry indexes are also included in Table 4.3. In the "Drug-Off" state, the mean first step length of the patients with mild PD is significantly shorter than that of the non-PD subjects (0.42 ± 0.11 vs. 0.55 ± 0.06, $p < 0.05$). The mean first step speed of the patients with mild PD is significantly slower than that of the non-PD subjects (0.90 ± 0.19 vs. 1.16 ± 0.27, $p < 0.05$). When compared to the non-PD subjects, the patients with mild PD in the "Drug-Off" state show a slight but non-significant reduction in first swing time. The symmetry indexes of the patients with mild PD are significantly larger than those of the non-PD subjects in first step length (16.36 ± 5.19 vs. 2.98 ± 4.40, $p < 0.01$), first swing time (10.98 ± 6.93 vs. 2.24 ± 2.73, $p < 0.01$), and first step speed (12.02 ± 6.92 vs. 3.81 ± 3.26, $p < 0.05$).

In the "Drug-On" state, the patients with mild PD demonstrate significant improvement in first step length (0.53 ± 0.07 vs. 0.42 ± 0.11, $p < 0.05$) as compared to the "Drug-Off" state. There are slight but non-significant increases in first swing time and first step speed. The patients with mild PD in the "Drug-On" state show no significant differences in any of the gait parameters when compared to the non-PD subjects. The symmetry indexes of the patients with mild PD in the "Drug-On" state are significantly greater than those of non-PD subjects in first step length (13.58 ± 8.58 vs. 2.98 ± 4.40, $p < 0.01$), first swing time (12.41 ± 9.88 vs. 2.24 ± 2.73, $p < 0.01$), and first step speed (16.81 ± 10.41 vs. 3.81 ± 3.26, $p < 0.01$). However, the patients with mild PD in the "Drug-On" state do not show significant improvement across all of the symmetry indexes when compared to the "Drug-Off" state.

4.4 Discussions

4.4.1 Differences during the steady-state walking period among patients with mild PD in the different states and non-PD subjects

Compared to the non-PD subjects, the patients with mild PD in the “Drug-Off” state during the steady-state walking period show significantly slower walking velocity, step speed and shorter step length. The quantitative outcomes obtained in this study are consistent with the findings of preceding studies [5, 15, 28, 83]. In the “Drug-On” state, the patients with mild PD show significant improvement in walking velocity and step speed; increases in step length are also observed as compared to the “Drug-Off” state. These results are also consistent with earlier studies [5, 74, 83-86]. It has been reported that the patients with mild PD in the “Drug-Off” state might exhibit an increase in cadence to compensate for the reduction in step length caused by the shuffling gait with small steps [87]; the patients with mild PD in the “Drug-On” state exhibit reductions in the stance phase and gait cycle time and an increase in walking velocity [88, 89]. However, in this study, a non-significant increase in cadence is observed in the patients with mild PD in the “Drug-On” state. Because the length of the pathway was limited, the patients with mild PD in the “Drug-On” state may not have taken enough steps to allow the detection of a significant reduction in cadence compared to the “Drug-Off” state. During the steady-state walking period, the non-PD show significant differences in the symmetry indexes to the patients with mild PD. The differences are assumed to be the results of the motor impairments in the patients with mild PD. Although the patients with mild PD in the “Drug-On” state exhibit improvement in most symmetry indexes when

compared to the “Drug-Off" state, there is no significant difference. There may be two plausible explanations. Since only one camera is used to collect the kinematic data (lateral view), the gait parameters of the left and right sides of the same participant are obtained from separate trials. Therefore, each symmetry index is the average of two trials; it can be assumed that the differences are also averaged, hence reducing potential significance. Besides, the patients with mild PD with different severity of neurodegeneration do not exhibit similar improvement in posture and balance control. According to the H&Y scale, only two PD patients show conspicuous improvement (from 3 to 2.5) in the “Drug-On” state, which is not sufficient to produce statistically significant improvements in the symmetry indexes.

Although the differences in gait parameters during the steady-state walking period between the non-PD and PD patients are observed and consistent with the preceding studies, the results suggest that it is not easy to recognize patients with mild PD due to the lack of statistical significance. However, at least four of the defined five associated symmetry indexes of the healthy are significantly better than those of the patients with mild PD, suggesting that the associated symmetry indexes derived from the steady state walking may facilitate the early detection and diagnosis of PD.

4.4.2 Differences during the gait initiation period among the patients with mild PD in the different states and non-PD subjects

Due to stooped posture and forward leaning, patients with mild PD may exhibit the following behavior: a significant forward ankle shift to reduce the backward center of foot pressure (COP)

shift, an increase in the unloading phase, a reduction in the vertical height of the first step, and a shortening in the length of the first step [6]. Breniere et al. have demonstrated that the reduction in the backward COP shift may decrease the COP forward acceleration of PD patients, hence reducing first step speed and step length during the gait initiation period [90]. Results from the quantitative analysis are consistent with the demonstration. Patients with mild PD exhibit significantly shorter first step and slower first step speed during the gait initiation period than the non-PD subjects.

When the patients with mild PD in different states are compared, the first step length in the "Drug-On" state is significantly increased. It has been reported that the proper levodopa dose can help the patients with mild PD increase their first step length and shorten the first swing phase by improving the performance in the unloading phase and the COP backward displacement [91]. The outcomes of this study are consistent with the previous findings, suggesting that the proposed system can provide useful information for identifying clinical improvement in gait initiation performance of patients with mild PD upon the administration of medication.

The patients with mild PD in the "Drug-On" state exhibit slight but insignificant improvement in the symmetry index of the first step length; moreover, their symmetry indexes of the first swing time and first step speed are worse but insignificant than those of the patients with mild PD in the "Drug-Off" state. Results indicate that levodopa treatment seems not to improve the symmetry indexes during the gait initiation period. In clinical observations, some patients with mild PD in the "Drug-On" state exhibit hesitation and freezing at gait onset unilaterally. Their first swing time and first step speed on the affected side were increased and reduced, respectively. The observations are

consistent with the prior studies [92, 93] that demonstrate motor symptoms including hesitation and freezing at gait onset may occur as the side effects of levodopa treatment. Although the results suggest that the symmetry indexes are not responsive to the levodopa treatment, it is insufficient to rule out that levodopa treatment facilitates the symmetry in gait during the gait initiation period. Further research is required to explain the effects of levodopa on gait symmetry during gait initiation.

During the gait initiation period, as compared to the patients with mild PD in both states, the non-PD subjects exhibit significantly greater performance in all of the symmetry indexes and few gait parameters. The results suggest that the identification of mild PD patient using the symmetry indexes during the gait initiation period may be easier than that using the gait parameters during the gait initiation period.

Due to the special demand for a decorated corridor, the identification of mild parkinsonian gait using the method introduced in chapter 3 may be not applicable in some clinics with small space. The results in this part of study provide another solution for identification of mild PD patient. Using the gait symmetry derived from the gait initiation period, clinicians may recognize patients with mild PD and monitor the improvement brought about by the medical treatment quickly and precisely. Besides, the crucial gait performances, including first step length, first swing time, and first step speed, are determined using the quantitative gait analysis outcomes and may facilitate the treatment management such as rehabilitation programs or drug.

4.5 Conclusion

The gait initiation and symmetry are indicators of gait performance and allow clinicians to comprehend contemporary gait performance of patients with Parkinson disease and to plan medical treatment or rehabilitation programs for them. In this study, a method using the CTA to track and analyze the gait initiation and symmetry of patients with mild PD is developed.

Using the CTA-based method, a number of quantitative gait parameters and associated symmetry indexes during the gait initiation and the steady-state walking period are derived, and the characteristics of mild parkinsonian gait then can be identified. Results reveal that the recognition of patients with mild PD can be attained using the quantitative gait symmetry indexes during the gait initiation period except those during the steady-state walking period. Because only a digital camera, space for subjects to perform gait initiation, two joint identifiers secured on a participant's the fibula head and lateral malleolus are required, this system presents promising portability and improved convenience for identification of patients with mild PD in clinics with small space or at home.

This study aims to assess the quantitative analysis of gait initiation and symmetry in walking of patients with mild PD, and therefore aid clinicians may detect and diagnose PD early and monitor the therapeutic effect from medical treatment or rehabilitation programs in clinics with small space; however, clinical applications can be expanded to analyze the motor performance of patients with other neuromuscular disorders.

Chapter 5 Conclusions & future studies

5.1 Conclusions

PD is a progressive neurodegenerative disease and the second most common neurodegenerative disorder after Alzheimer's disease and is expected to impose an increasing social and economic burden on societies as people age. The diagnosis and treatment of PD in the early stages therefore becomes an important issue. The diagnosis of PD is based on the presence of the classic clinical signs: resting tremor, rigidity, postural instability, and bradykinesia. However, the clinical presentation and progression can be greatly variable. The identification of characteristics may be difficult thereby, especially in the early stages of PD. Gait disturbance presents a cardinal motor symptom and may be observed in early stages of the disease; therefore, the quick and precise recognition of mild PD patient, the quantification of the mild parkinsonian gait performance, and the improvements provided by the treatment regime or rehabilitation programs are important references and may aid the early diagnosis and the following treatment management. However, the recognition and quantification of mild parkinsonian gait have been hindered due to the lack of tools that can provide prompt gait analysis, facilitate data collection and gait analysis, and lower a patient's level of exertion during the examinations, especially be installed in clinics or at home,.

To address the demand, we attempted to develop solutions that require simple clinical settings and can be easily installed and used in a clinic or at home with limited space to quantify and recognize mild PD parkinsonian gait, and further evaluate the therapeutic effect of L-dopa on PD

patients. In this proposed research, two video-based gait analysis methods that are different from traditional sensor- or marker-based approaches are developed in the 1st and 2nd phases, respectively.

During the 1st phase, a portable and convenient video-based method using KPCA to recognize and quantify mild parkinsonian gait during the steady-state walking period was developed and implemented. The method requires only a decorated corridor and a digital camera capturing people's lateral silhouette during walking so that it can be easily deployed in clinics with space or budgetary limitations. The time and cost for data collection and gait analysis therefore become less than the conventional sensor- or marker-based approaches that request a user to wear sensors or a specific suit.

The proposed method uses the KPCA to reduce the dimensionality of image frames and therefore the computational cost for post-processing can be effectively reduced. The kernel principal components from a walking image frame sequence are used to form a biometric feature vector to represent a given participant. After observation and comparison, we found that the moment of occurrence of the heel strike can be determined using the primary KPCA component (1st KPC) waveforms. We are able to reconstruct each participant's gait profile for follow-up recognition and quantification thereby.

The recognition sensitivity of the method was compared with other competing methods, the area feature and PCA-based feature approaches. Although there are few significant differences among the gait patterns, the proposed method using KPCA presents an encouraging sensitivity of 80.51% in classifying subjects in different states, much better than the competing area feature

(50.16%) and PCA-based (69.44%) approaches. The quantitative results show that PD patients who receive the L-dopa treatment show improvement in their gait cycle time, stride length, walking velocity, cadence, and step frequency. The correlations between the five UPDRS part III sub-scores and the derived gait parameters show that four gait parameters are significantly correlated with at least limb akinesia, rigidity and tremor, indicating that it is possible to evaluate the motor deviation of the patients with mild PD through the derived gait parameters. In addition, the proposed approach provides the power spectrum of the participant's gait as additional information to analyze the irregularity of the motions of patients with mild PD.

It may be a problem for clinics with small space to deploy the 1st method requiring a decorated corridor. Therefore, during the 2nd phase, a video-based method using the CTA was developed and implemented to track and analyze the gait initiation and symmetry of patients with mild PD. The method use a digital camcorder and joint identifiers secured at palpable anatomic landmarks, the fibula head and lateral malleolus, to capture the knee and ankle joint movements by which the heel strike and toe off events can be determined. A participant's gait pattern then can be reconstructed and the gait performance and associated symmetry indexes during the gait initiation and steady-state walking periods can be evaluated thereby.

During both the gait initiation and steady-state walking periods, the PD patients who received L-dopa treatment show improvement in gait parameters, proving the therapeutic effect of the L-dopa treatment demonstrated in [91]. Same as the 1st phase, the improvement brought about by the L-dopa treatment was not robust on the patients with mild PD, resulting in a difficulty in

identifying differences between the patients with mild PD in the “Drug-Off” and “Drug-On” states. However, results show that the gait symmetry indexes derived from the gait initiation period may also facilitate the identification of patients with mild PD.

Compared to the KPCA-based method, the CTA-based method provides a solution requiring a smaller space and a simpler clinical setting for early detection and diagnosis of PD. Besides, quantitative analysis of gait performance is also attained for monitoring the progression of PD and improvement brought about by the rehabilitation programs and drug administration.

The study presents two techniques for clinicians and researchers with which to detect and diagnose PD early and assess the progression of PD using gait patterns recorded in monocular image frames. Although the proposed methods currently aim to recognize and quantify the mild parkinsonian gait, clinical applications can be expanded to analyze the gait performance of patients with other neuromuscular disorders in future.

5.2 Recommendations for future studies

This study is not perfect due to some intrinsic limitations. Therefore, here are some recommendations for future studies. An orientation or a pre-education program for clinical setting, safety, and identification of the palpable anatomic landmarks can facilitate the use of the CTA-based method without skilled personnel. Moreover, there is a lack of patients with advanced motor symptoms in this study, the therapeutic effect of prescribed L-dopa treatment on the PD patients seems to be not robust and thereby it resulted in insignificant improvement in walking

symmetry of the PD patients. Further researches are required to explain the effects of L-dopa treatment on the walking symmetry and gait performance of PD patients.

Abbreviations:

PD is Parkinson's disease.

VTA is ventral tegmental area.

KPCA is kernel-based principal component analysis.

UPDRS is Unified Parkinson's Disease Rating Scale.

L-dopa is levodopa.

MDC is minimum distance classifier.

DFT is discrete Fourier transform.

PCA is principal component analysis.

^{1st}***KPC*** is the magnitude of the first principal component.

LSD is least significant difference.

CTA is centroid tracking algorithm.

LEDD is levodopa at an equivalent daily dose.

H&Y is Hoehn & Yahr.

SI is symmetry index.

References:

[1] J. Parkinson, "An essay on the shaking palsy," *Journal of Neuropsychiatry and Clinical Neurosciences,* vol. 14, pp. 223-236, 2002.

[2] L. M. L. de Lau and M. Breteler, "Epidemiology of Parkinson's disease," *The Lancet Neurology,* vol. 5, pp. 525-535, 2006.

[3] R. Spehlmann and S. M. Stahl, "Dopamine acetyllcholine imbalance in Parkinson's disease: possible regenerative overgrowth of cholinergic axon terminals," *The Lancet,* vol. 307, pp. 724-726, 1976.

[4] M. Hong, G. Earhart, D. Damiano, and J. Perlmutter, "Decreased Arm Swing At Fast Walking Speed in Mild Parkinson Disease (Pd)," *Journal of Neurologic Physical Therapy,* vol. 29, pp. 209-210, 2005.

[5] A. Salarian, H. Russmann, F. J. G. Vingerhoets, C. Dehollain, Y. Blanc, P. R. Burkhard, and K. Aminian, "Gait assessment in Parkinson's disease: toward an ambulatory system for long-term monitoring," *IEEE Transactions on Biomedical Engineering,* vol. 51, pp. 1434-1443, 2004.

[6] S. E. Halliday, D. A. Winter, J. S. Frank, A. E. Patla, and F. Prince, "The initiation of gait in young, elderly, and Parkinson's disease subjects," *Gait & posture,* vol. 8, pp. 8-14, 1998.

[7] http://medchrome.com.

[8] J. Jankovic, "Pathophysiology and clinical assessment of motor symptoms in Parkinson's disease," *Handbook of Parkinson's disease,* vol. 2, pp. 129-157, 1987.

[9] P. Krack, A. Benazzouz, P. Pollak, P. Limousin, B. Piallat, D. Hoffmann, J. Xie, and A. L. Benabid, "Treatment of tremor in Parkinson's disease by subthalamic nucleus stimulation," *Movement disorders,* vol. 13, pp. 907-914, 1998.

[10] M. H. Sharpe, S. A. Cermak, and D. S. Sax, "Motor planning in Parkinson patients," *Neuropsychologia,* vol. 21, pp. 455-462, 1983.

[11] W. C. Roller, S. Glatt, B. Vetere-Overfield, and R. Hassanein, "Falls and Parkinson's disease," *Clinical neuropharmacology,* vol. 12, pp. 98-105, 1989.

[12] Y. A. M. Grimbergen, M. Munneke, and B. R. Bloem, "Falls in Parkinson's disease," *Current opinion in neurology,* vol. 17, pp. 405-415, 2004.

[13] L. Coughlin and J. Templeton, "Hip fractures in patients with Parkinson's disease," *Clinical Orthopaedics and Related Research,* vol. 148, pp. 192-195, 1980.

[14] O. Blin, A. M. Ferrandez, and G. Serratrice, "Quantitative analysis of gait in Parkinson patients: increased variability of stride length," *Journal of the neurological sciences,* vol. 98, pp. 91-97, 1990.

[15] E. Knutsson, "An analysis of parkinsonian gait," *Brain,* vol. 95, p. 475, 1972.

[16] M. Murray, S. Sepic, G. Gardner, and W. Downs, "Walking patterns of men with parkinsonism," *American journal of physical medicine,* vol. 57, p. 278, 1978.

[17] M. E. Morris, F. Huxham, J. McGinley, K. Dodd, and R. Iansek, "The biomechanics and

motor control of gait in Parkinson disease," *Clinical Biomechanics,* vol. 16, pp. 459-470, 2001.

[18] J. Jankovic, "Parkinson's disease: clinical features and diagnosis," *Journal of Neurology, Neurosurgery & Psychiatry,* vol. 79, p. 368, 2008.

[19] R. N. Stauffer, E. Chao, and A. Gyory, "Biomechanical gait analysis of the diseased knee joint," *Clin Orthop,* vol. 126, pp. 246-255, 1977.

[20] J. E. Cutting and L. T. Kozlowski, "Recognizing friends by their walk: Gait perception without familiarity cues," *Bulletin of the Psychonomic Society,* vol. 9, pp. 353-356, 1977.

[21] J. E. Cutting, D. R. Proffitt, and L. T. Kozlowski, "A biomechanical invariant for gait perception," *Journal of Experimental Psychology: Human Perception and Performance,* vol. 4, pp. 357-372, 1978.

[22] L. T. Kozlowski and J. E. Cutting, "Recognizing the sex of a walker from a dynamic point-light display," *Attention, Perception, & Psychophysics,* vol. 21, pp. 575-580, 1977.

[23] J. P. Hubble, R. Pahwa, D. K. Michalek, C. Thomas, and W. C. Koller, "Interactive video conferencing: a means of providing interim care to Parkinson's disease patients," *Movement disorders,* vol. 8, pp. 380-382, 1993.

[24] A. Lozano, A. Lang, N. Galvez-Jimenez, J. Miyasaki, J. Duff, W. Hutchison, and J. Dostrovsky, "Effect of GPi pallidotomy on motor function in Parkinson's disease," *The Lancet,* vol. 346, pp. 1383-1387, 1995.

[25] T. Kepple, S. Stanhope, K. Lohmann, and N. Roman, "A video-based technique for measuring ankle--subtalar motion during stance," *Journal of biomedical engineering,* vol. 12, pp. 273-280, 1990.

[26] M. Swider, "The application of video image processing to quantitative analysis of extremity tremor in humans," *Journal of Neuroscience Methods,* vol. 84, pp. 167-172, 1998.

[27] L. G. Chang, JA Burne, R., "An automated form of video image analysis applied to classification of movement disorders," *Disability & Rehabilitation,* vol. 22, pp. 97-108, 2000.

[28] Y. R. Yang, Y. Y. Lee, S. J. Cheng, P. Y. Lin, and R. Y. Wang, "Relationships between gait and dynamic balance in early Parkinson's disease," *Gait & posture,* vol. 27, pp. 611-615, 2008.

[29] R. Okuno, S. Fujimoto, J. Akazawa, M. Yokoe, S. Sakoda, and K. Akazawa, "Analysis of spatial temporal plantar pressure pattern during gait in Parkinson's disease," in *30th Annual International Conference of the IEEE* Vancouver, BC 2008, pp. 1765-1768.

[30] M. Benedetti, F. Catani, A. Leardini, E. Pignotti, and S. Giannini, "Data management in gait analysis for clinical applications," *Clinical Biomechanics,* vol. 13, pp. 204-215, 1998.

[31] H. Chang, T. Chuang, S. Lee, S. Liao, H. Lee, Y. Shih, and H. Cheng, "Temporal differences in relative phasing of gait initiation and first step length in patients with cervical and lumbosacral spinal cord injuries," *Spinal cord,* vol. 42, pp. 281-289, 2004.

[32] C. Cho, Y. Osaki, M. Kunin, B. Cohen, C. W. Olanow, and T. Raphan, "A Model-Based

Approach for Assessing Parkinsonian Gait and Effects of Levodopa and Deep Brain Stimulation," in *Proceedings of the 28th IEEE EMBS Annual International Conference*, Nwe York City, 2006, pp. 1228-1231.

[33] P. S. Huang, C. J. Harris, and M. S. Nixon, "Human gait recognition in canonical space using temporal templates," *IEE Proceedings of Vision, Image and Signal Processing,* vol. 146, pp. 93-100, 1999.

[34] M. S. Nixon, J. N. Carter, M. G. Grant, L. Gordon, and J. B. Hayfron-Acquah, "Automatic recognition by gait: progress and prospects," *Sensor Review,* vol. 23, pp. 323-331, 2003.

[35] J. Little and J. Boyd, "Recognizing people by their gait: the shape of motion," *Videre: Journal of Computer Vision Research,* vol. 1, pp. 1-32, 1998.

[36] S. A. Niyogi and E. H. Adelson, "Analyzing and recognizing walking figures in XYT," in *IEEE Proceedings of Computer Society Conference on Computer Vision and Pattern Recognition (CVPR'94)*, 1994, pp. 469-474.

[37] H. Murase and R. Sakai, "Moving object recognition in eigenspace representation: gait analysis and lip reading," *Pattern recognition letters,* vol. 17, pp. 155-162, 1996.

[38] P. S. Huang, C. J. Harris, and M. S. Nixon, "Recognising humans by gait via parametric canonical space," *Artificial Intelligence in Engineering,* vol. 13, pp. 359-366, 1999.

[39] B. Scholkopf, A. Smola, and K. R. Muller, "Nonlinear component analysis as a kernel eigenvalue problem," *Neural computation,* vol. 10, pp. 1299-1319, 1998.

[40] K. Polat and S. Gunes, "Automatic determination of diseases related to lymph system from lymphography data using principles component analysis (PCA), fuzzy weighting pre-processing and ANFIS," *Expert Systems with Applications,* vol. 33, pp. 636-641, 2007.

[41] J. Yang, D. Zhang, and A. F. Frangi, "Two-dimensional PCA: a new approach to appearance-based face representation and recognition," *Pattern Analysis and Machine Intelligence, IEEE Transactions on,* vol. 26, pp. 131-137, 2004.

[42] H. Kong, L. Wang, E. K. Teoh, X. Li, J. G. Wang, and R. Venkateswarlu, "Generalized 2D principal component analysis for face image representation and recognition," *Neural Networks,* vol. 18, pp. 585-594, 2005.

[43] Q. Du and J. E. Fowler, "Hyperspectral image compression using JPEG2000 and principal component analysis," *Geoscience and Remote Sensing Letters, IEEE,* vol. 4, pp. 201-205, 2007.

[44] N. Kambhatla and T. K. Leen, "Dimension reduction by local principal component analysis," *Neural computation,* vol. 9, pp. 1493-1516, 1997.

[45] W. Zhao, R. Chellappa, and A. Krishnaswamy, "Discriminant analysis of principal components for face recognition," 1998, pp. 336-341.

[46] R. L. Tatusov, D. A. Natale, I. V. Garkavtsev, T. A. Tatusova, U. T. Shankavaram, B. S. Rao, B. Kiryutin, M. Y. Galperin, N. D. Fedorova, and E. V. Koonin, "The COG database: new developments in phylogenetic classification of proteins from complete genomes," *Nucleic acids research,* vol. 29, pp. 22-28, 2001.

[47] T. Sato, "Application of principal-component analysis on near-infrared spectroscopic data of vegetable oils for their classification," *Journal of the American Oil Chemists' Society,* vol. 71, pp. 293-298, 1994.

[48] J. Khan, J. S. Wei, M. Ringnér, L. H. Saal, M. Ladanyi, F. Westermann, F. Berthold, M. Schwab, C. R. Antonescu, and C. Peterson, "Classification and diagnostic prediction of cancers using gene expression profiling and artificial neural networks," *Nature medicine,* vol. 7, pp. 673-679, 2001.

[49] A. Krauze and R. I. Zalewski, "Classification of honeys by principal component analysis on the basis of chemical and physical parameters," *Zeitschrift für Lebensmitteluntersuchung und-Forschung A,* vol. 192, pp. 19-23, 1991.

[50] M. Turk and A. Pentland, "Eigenfaces for recognition," *Journal of cognitive neuroscience,* vol. 3, pp. 71-86, 1991.

[51] D. L. Ruderman, "Origins of scaling in natural images," *Vision research,* vol. 37, pp. 3385-3398, 1997.

[52] R. Rosin, H. Topka, and J. Dichgans, "Gait initiation in Parkinson's disease," *Movement disorders,* vol. 12, pp. 682-690, 1997.

[53] S. T. Moore, H. G. MacDougall, and W. G. Ondo, "Ambulatory monitoring of freezing of gait in Parkinson's disease," *Journal of Neuroscience Methods,* vol. 167, pp. 340-348, 2008.

[54] L. Fuyuan, W. Jue, and H. Ping, "Multi-resolution entropy analysis of gait symmetry in neurological degenerative diseases and amyotrophic lateral sclerosis," *Med Eng Phys,* vol. 30, pp. 299-310, 2008.

[55] D. J. Gelb, E. Oliver, and S. Gilman, "Diagnostic criteria for Parkinson disease," *Archives of neurology,* vol. 56, pp. 33-39, 1999.

[56] A. Burleigh Jacobs, F. B. Horak, J. G. Nutt, and J. A. Obeso, "Step initiation in Parkinson's disease: influence of levodopa and external sensory triggers," *Movement disorders,* vol. 12, pp. 206-215, 1997.

[57] W. Herzog, B. M. Nigg, L. J. Read, and E. Olsson, "Asymmetries in ground reaction force patterns in normal human gait," *Medicine and science in sports and exercise,* vol. 21, pp. 110-114, 1989.

[58] P. Meir, G. Nir, B. Yacov, and P. Chava, "Is freezing of gait in Parkinson's disease related to asymmetric motor function?," *Ann Neurol,* vol. 57, pp. 656-663, 2005.

[59] J. Chodera, "Analysis of gait from footprints," *Physiotherapy,* vol. 60, pp. 179-181, 1974.

[60] J. Chodera and R. Levell, "Footprint patterns during walking," *Perspectives in biomedical engineering,* pp. 81–90, 1973.

[61] H. Law, "Microcomputer-based low-cost method for measurement of spatial and temporal parameters of gait," *Journal of biomedical engineering,* vol. 9, pp. 115-120, 1987.

[62] P. Allard, R. Lachance, R. Aissaoui, and M. Duhaime, "Simultaneous bilateral 3-D able-bodied gait," *Human Movement Science,* vol. 15, pp. 327-346, 1996.

[63] D. J. STEFANYSHYN and J. R. ENGSBERG, "Right to left differences in the ankle joint

complex range of motion," *Medicine & Science in Sports & Exercise,* vol. 26, pp. 551-555, 1994.

[64] E. Oron, A. Kumar, and Y. Bar-Shalom, "Precision tracking with segmentation for imaging sensors," *IEEE Transactions on Aerospace and Electronic Systems,* vol. 29, pp. 977-987, 1993.

[65] V. Naidu, G. Girija, and J. Raol, "Centroid Tracking and Target Identity Estimation using Image Sensor Data," National Aerospace Laboratories2005.

[66] A. Lang and A. Lozano, "Parkinson's disease. Second of two parts," *The New England journal of medicine,* vol. 339, pp. 1130-1143, 1998.

[67] P. Martinez Martin, A. Gil Nagel, L. M. Gracia, J. B. Gomez, J. Martinez Sarries, and F. Bermejo, "Unified Parkinson's disease rating scale characteristics and structure," *Movement disorders,* vol. 9, pp. 76-83, 1994.

[68] S. Sarkar, P. J. Phillips, Z. Liu, I. R. Vega, P. Grother, and K. W. Bowyer, "The human ID gait challenge problem: Data sets, performance, and analysis," *IEEE transactions on pattern analysis and machine intelligence,* pp. 162-177, 2005.

[69] S.-T. Bow, *Pattern Recognition and Image Preprocessing*, 2nd ed.: Marcel Dekker, Inc. New York, NY, USA, 2002.

[70] R. O. Duda, P. E. Hart, and D. G. Stork, *Pattern classification*, 2nd ed.: New York: John Wiley & Sons, 2000.

[71] L. Wang, T. Tan, H. Ning, and W. Hu, "Silhouette analysis-based gait recognition for human identification," *IEEE transactions on pattern analysis and machine intelligence,* pp. 1505-1518, 2003.

[72] E. O. Brigham, *The fast Fourier transform and its applications.*: Englewood Cliffs, N.J.: Prentice Hall., 1988.

[73] J. D. O'Sullivan, C. M. Said, L. C. Dillon, M. Hoffman, and A. J. Hughes, "Gait analysis in patients with Parkinson's disease and motor fluctuations: influence of levodopa and comparison with other measures of motor function," *Mov Disord,* vol. 13, pp. 900-6, 1998.

[74] M. Vokaer, N. A. Azar, and D. Z. de Beyl, "Effects of levodopa on upper limb mobility and gait in Parkinson's disease," *Journal of Neurology, Neurosurgery & Psychiatry,* vol. 74, p. 1304, 2003.

[75] S. Lubik, W. Fogel, V. Tronnier, M. Krause, J. Konig, and W. Jost, "Gait analysis in patients with advanced Parkinson disease: different or additive effects on gait induced by levodopa and chronic STN stimulation," *Journal of neural transmission,* vol. 113, pp. 163-173, 2006.

[76] A. Salarian, H. Russmann, F. J. Vingerhoets, C. Dehollain, Y. Blanc, P. R. Burkhard, and K. Aminian, "Gait assessment in Parkinson's disease: toward an ambulatory system for long-term monitoring," *IEEE Trans Biomed Eng,* vol. 51, pp. 1434-1443, Aug 2004.

[77] C. W. Cho, W. H. Chao, S. H. Lin, and Y. Y. Chen, "A vision-based analysis system for gait recognition in patients with Parkinson's disease," *Expert Systems with Applications,* vol. 36, pp. 7033-7039, 2009.

[78] M. M. Hoehn and M. D. Yahr, "Parkinsonism: Onset, progression and mortality," *Neurology,* 2001.

[79] J. M. Jasiewicz, J. H. J. Allum, J. W. Middleton, A. Barriskill, P. Condie, B. Purcell, and R. C. T. Li, "Gait event detection using linear accelerometers or angular velocity transducers in able-bodied and spinal-cord injured individuals," *Gait & posture,* vol. 24, pp. 502-509, 2006.

[80] R. O. Robinson, W. Herzog, and B. M. Nigg, "Use of force platform variables to quantify the effects of chiropractic manipulation on gait symmetry," *J Manip Physiol Ther,* vol. 10, pp. 172-176, 1987.

[81] E. B. Titianova and I. M. Tarkka, "Asymmetry in walking performance and postural sway in patients with chronic unilateral cerebral infarction," *J Rehabil Res Dev,* vol. 32, pp. 236-244, 1995.

[82] C. M. Kim and J. J. Eng, "Symmetry in vertical ground reaction force is accompanied by symmetry in temporal but not distance variables of gait in persons with stroke," *Gait & posture,* vol. 18, pp. 23-28, 2003.

[83] M. Ferrarin, L. Lopiano, M. Rizzone, M. Lanotte, B. Bergamasco, M. Recalcati, and A. Pedotti, "Quantitative analysis of gait in Parkinson's disease: a pilot study on the effects of bilateral sub-thalamic stimulation," *Gait & posture,* vol. 16, pp. 135-148, 2002.

[84] P. Krystkowiak, J.-L. Blatt, J.-L. Bourriez, A. Duhamel, M. Perina, S. Blond, J.-D. Guieu, A. Destee, and L. Defebvre, "Effects of subthalamic nucleus stimulation and levodopa treatment on gait abnormalities in Parkinson disease," *Arch Neurol,* vol. 60, pp. 80-84, 2003.

[85] S. Lubik, W. Fogel, V. Tronnier, M. Krause, J. König, and W. H. Jost, "Gait analysis in patients with advanced Parkinson disease: different or additive effects on gait induced by levodopa and chronic STN stimulation," *J Neural Transm,* vol. 113, pp. 163-173, 2006.

[86] J. D. O'Sullivan, C. M. Said, L. C. Dillon, M. Hoffman, and A. J. Hughes, "Gait analysis in patients with Parkinson's disease and motor fluctuations: influence of levodopa and comparison with other measures of motor function," *Movement disorders,* vol. 13, pp. 900-906, 1998.

[87] M. E. Morris, R. Iansek, T. A. Matyas, and J. J. Summers, "The pathogenesis of gait hypokinesia in Parkinson's disease," *Brain,* vol. 117, pp. 1169-1181, 1994.

[88] K. L. Siegel and L. V. Metman, "Effects of bilateral posteroventral pallidotomy on gait of subjects with Parkinson disease," *Arch Neurol,* vol. 57, pp. 198-204, 2000.

[89] M. Ferrarin, M. Rizzone, L. Lopiano, M. Recalcati, and A. Pedotti, "Effects of subthalamic nucleus stimulation and L-dopa in trunk kinematics of patients with Parkinson's disease," *Gait & posture,* vol. 19, pp. 164-171, 2004.

[90] Y. Breniere, M. C. Do, and S. Bouisset, "Are dynamic phenomena prior to stepping essential to walking?," *J Mot Behav,* vol. 19, pp. 62-76, 1987.

[91] P. Crenna, I. Carpinella, M. Rabuffetti, M. Rizzone, L. Lopiano, M. Lanotte, and M. Ferrarin, "Impact of subthalamic nucleus stimulation on the initiation of gait in Parkinson's disease,"

Exp Brain Res, vol. 172, pp. 519-532, 2006.

[92] N. Giladi, D. McMahon, S. Przedborski, E. Flaster, S. Guillory, V. Kostic, and S. Fahn, "Motor blocks in Parkinson's disease," *Neurology,* vol. 42, pp. 333-339, 1992.

[93] L. M. Ambani and M. H. Van Woert, "Start hesitation-a side effect of long-term levodopa therapy," *New England Journal of Medicine,* vol. 288, pp. 1113-1115, 1973.

[94] M. M. Hoehn and M. D. Yahr, "Parkinsonism: Onset, progression and mortality," *Neurology,* vol. 57, pp. S11-S26, 2001.

[95] G. C. e. al., "The Unified Parkinson's Disease Rating Scale (UPDRS): Status and recommendations," *Movement disorders,* vol. 18, pp. 738-750, 2003.

[96] S. Fahn, R. Elton, and U. D. Committee, "Unified Parkinson's disease rating scale," *Recent developments in Parkinson's disease,* vol. 2, pp. 153-163, 1987.

[97] P. Martinez-Martin, A. Gil-Nagel, L. Morlan Gracia, J. Balseiro Gomez, J. Martinez-Sarries, and F. Bermejo, "Unified Parkinson's disease rating scale characteristics and structure," *Movement disorders,* vol. 9, pp. 76-83, 1994.

[98] C. Ramaker, J. Marinus, A. M. Stiggelbout, and B. J. van Hilten, "Systematic evaluation of rating scales for impairment and disability in Parkinson's disease," *Movement disorders,* vol. 17, pp. 867-876, 2002.

[99] M. Richards, K. Marder, L. Cote, and R. Mayeux, "Interrater reliability of the Unified Parkinson's Disease Rating Scale motor examination," *Mov Disord,* vol. 9, pp. 89-91, 1994.

[100] K. Shaw, A. Lees, and G. Stern, "The impact of treatment with levodopa on Parkinson's disease," *QJM,* vol. 49, p. 283, 1980.

[101] A. Rajput, B. Rozdilsky, A. Rajput, and L. Ang, "Levodopa efficacy and pathological basis of Parkinson syndrome," *Clinical neuropharmacology,* vol. 13, pp. 553-558, 1990.

[102] M. Stacy and A. G. DO, "Optimizing long-term therapy for Parkinson disease: levodopa, dopamine agonists, and treatment-associated dyskinesia," *Clinical neuropharmacology,* vol. 31, p. 51, 2008.

[103] F. J. G. Vingerhoets, J. G. Villemure, P. Temperli, C. Pollo, E. Pralong, and J. Ghika, "Subthalamic DBS replaces levodopa in Parkinson's disease," *Neurology,* vol. 58, pp. 396-401, 2002.

[104] H. B. Menz, M. D. Latt, A. Tiedemann, M. Mun San Kwan, and S. R. Lord, "Reliability of the GAITRite walkway system for the quantification of temporo-spatial parameters of gait in young and older people," *Gait & posture,* vol. 20, pp. 20-25, 2004.

[105] R. Baker, "Gait analysis methods in rehabilitation," *Journal of NeuroEngineering and Rehabilitation,* vol. 3, pp. 4-13, 2006.

Appendix A: Assessment of treatment of parkisonism

A.1 Assessment of Parkinson's disease

Hand-writing samples, speech analysis, and questions that focus on developing symptomatology can be used in the preclinical stage to detect early manifestations of PD. An estimation of the stage and severity of the disease can be made using a staging scale. The two most widely used are the Hoehn and Yahr classification of disability scale (H&Y stage) and the unified Parkinson's disease rating scale (UPDRS).

A.1.1 Hoehn and Yahr scale

The Hoehn and Yahr scale is a rating scale for describing how the symptoms of PD progress [94]. The current scale includes stages 0 through 5 to indicate the relative level of disability, and stages 1.5 and 2.5 are proposed to reflect the growing knowledge of PD-related impairments.

- Stage 0: No signs of disease.
- Stage 1: Unilateral symptoms only.
- Stage 1.5: Unilateral and axial involvement.
- Stage 2: Bilateral symptoms. No impairment of balance.
- Stage 2.5: Mild bilateral disease with recovery on pull test.
- Stage 3: Balance impairment. Mild to moderate disease. Physically independent.
- Stage 4: Severe disability, but still able to walk or stand unassisted.

- Stage 5: Needing a wheelchair or bedridden unless assisted.

A.1.2 Unified Parkinson's Disease Rating Scale (UPDRS)

Due to the disagreements in rating PD-related disability and impairment using different Parkinson's disease rating scales such as intermediate scale for assessment of PD (ISAPD) and Schwab and England scale (SES), the UPDRS was developed to address the demand of incorporating elements from earlier scales to provide a compound but comprehensive scale to capture multiple aspects of PD [67, 95-97]. At present, the UPDRS is the most widely used clinical tool for the assessment of parkinsonian motor impairment and disability [98]. The UPDRS reviewed and modified by a consortium of movement disorders specialists comprises four main sections as the following:

- Part I: evaluation of mentation, behavior, and mood.
- Part II: self evaluation of the activities of daily life (ADLs) including speech, swallowing, handwriting, dressing, hygiene, falling, salivating, turning in bed, walking, cutting food.
- Part III: clinician-scored motor evaluation;
- Part IV: Complications of therapy.

The UPDRS is often accompanied by and reported with such scales as the "Schwab and England scale" or the "Hoehn and Yahr scale", whereas the latter scales are not parts of the UPDRS. The UPDRS strongly relies on the experience or the expertise of clinician and therefore the interpretation may vary due to individual subjective judgments or opinions. Richard et al. indicated

the disagreement between the UPDRS raters despite that the scale is the most common and uniform tool that captures multiple aspects of PD [99].

A.2 Treatment of Parkinson's disease

Although the physician, therapist, and neurologist cooperatively institute medical program against PD, a cure for the progressive disease is currently not available. However, the effects of the disease and secondary impairments can be minimized using early and vigorous treatment.

A.2.1 Levodopa

Levodopa (L-dopa) is the most preferred and effective drug treatment for PD and is administrated orally with carbidopa. It is a metabolic precursor of dopamine that can raise the level of striatal dopamine in the basal ganglia and maintain the equilibrium between dopamine and acetylcholine. The primary benefit is to alleviate bradykinesia and rigidity, but less effect on resting tremor. However, long-term use of L-dopa therapy may result in a deterioration of the drug's overall therapeutic effectiveness. The depletion of the therapeutic effectiveness is most likely due to a progressive decrease in responsiveness of the dopamine receptors or to progressive loss of dopamine neurons in substantia nigra. The detailed description and efficacy of L-dopa can be found in [93, 100-102].

A.2.2 Deep brain stimulation (DBS)

Deep brain stimulation (DBS) is a surgical procedure used to replace drug treatment and

alleviate the symptoms of PD, such as tremor, rigidity, stiffness, bradykinesia, and abnormal gait pattern. The detailed descriptions and efficacy can be found in [103]. DBS uses a neurostimulator, a battery-operated medical device that is surgically implanted into a deep brain region to deliver electrical stimulation to targeted areas in the brain that control movement, blocking the abnormal nerve signals that cause tremor and PD motor symptoms. Generally, these targets are the thalamus, subthalamic nucleus, and globus pallidus.

The DBS system consists of three components: the lead, the extension, and the neurostimulator. The lead (an electrode), which is a thin and insulated wire, is inserted through a small hole in the skull and implanted in the brain. The tip of the electrode is positioned within the targeted brain area. The extension is an insulated wire that is passed under the skin of the head, neck, and shoulder, connecting the lead to the neurostimulator. The neurostimulator is the third component and is usually implanted under the skin near the collarbone or lower in the chest, sometimes under the skin over the abdomen. Once the system is in place, electrical impulses are sent from the neurostimulator up along the extension wire and the lead and into the brain. These impulses interfere with and block the disordered neural signals that cause PD symptoms.

Appendix B: Comparing the KPCA-based feature approach with the GAITRite® method for validation

To evaluate the validity of the proposed KPCA-based method in quantifying gait performance to aid clinical diagnoses and further applications, the quantitative gait parameters from the proposed approach were compared with the outcomes of the GAITRite® system (CIR system, Inc., USA) prior to the actual experiment.

The GAITRite® system is an instrumented walkway system that has been validated as a reliable tool for the measurement of kinematic gait parameters [104]. Six healthy male volunteers with an average age of 54 years (max = 76.5 years, min = 46 years, S.D. = 9.7 years) were recruited, and they provided informed consent for participation. Using an identical experimental setup to that employed in the present study, these volunteers were asked to perform four walking trials at their natural pace, and a total of 24 trials were collected.

Figure B1 shows the equipment setup used to perform the concurrent gait analysis by the GAITRite- and KPCA-based methods.

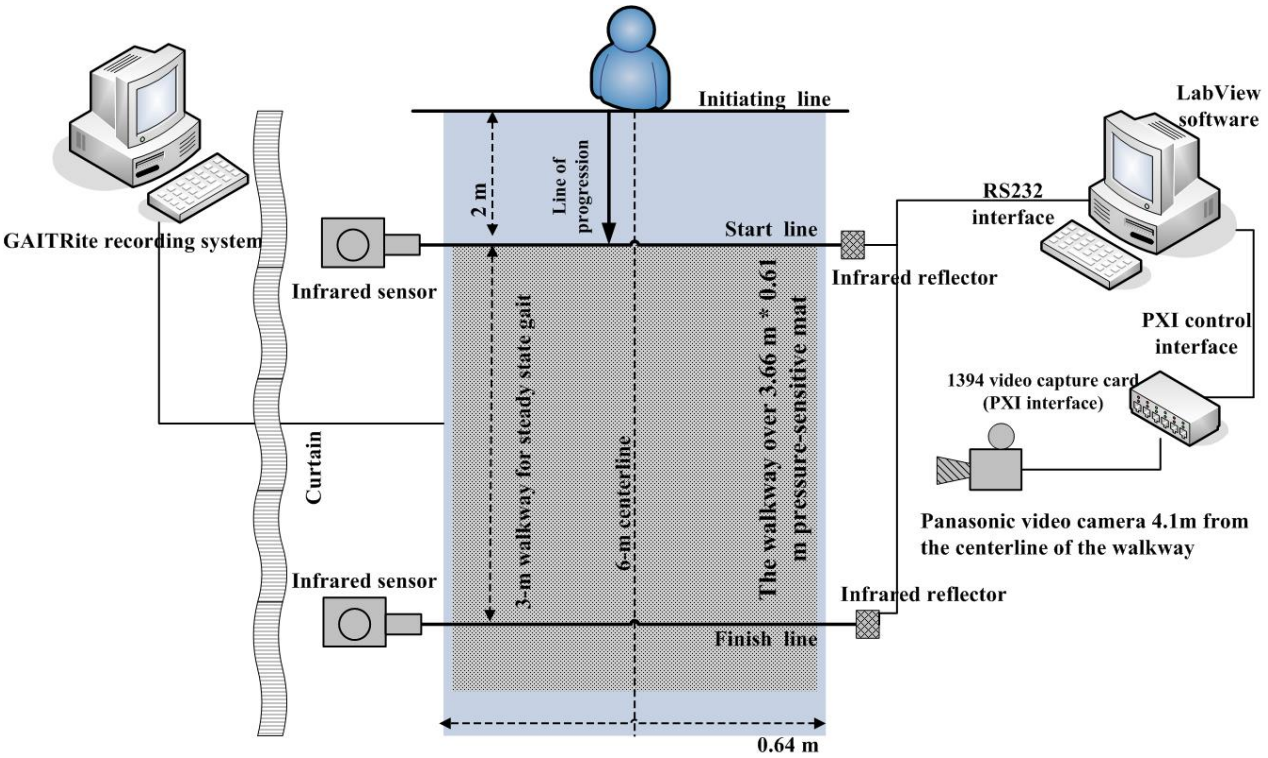

Figure B1. Equipment setup used to measure the gait parameters with the GAITRite® mat and recording system along with the video methods.

Gait analysis was performed using an electrical spatial and temporal analysis system (GAITRite® system; CIR Systems Inc., Clifton, NJ, USA). The GAITRite® system is a 4.6-m-long electronic walkway that connects to the serial port (19,200 baud rate) of a windows XP computer. The walkway is 1/8 inch thick and contains 16,128 sensors sandwiched between a thin vinyl cover on top and a rubber bottom. The active senor area is 0.61 m wide by 3.66 m long. GAITRite® software (ver. 3.8) was used to process the footstep data and to provide quantified temporal and spatial parameters.

The Panasonic video camera (model PV-GS400) used to videotape the walking trials was mounted on a tripod and positioned midway between the start and finish lines of the walkway, with the camera's field of view perpendicular to the long axis of the walkway. All trials were videotaped

using a sampling rate of 15 image frames per second and an image size of 320 × 240 pixels. The plane of the camera's shutter was located 4.1 m from the centerline of the walkway. The size of the field of view ensured that two pairs of infrared sensors, which were aligned with the start and finish lines, could be seen in the camera's viewfinder. One graphical programming utility was developed using the NI LabVIEW environment (LabVIEW 8.5, National Instruments, Austin, TX, U.S.A) and a 1394 video capture card (Model PXI-8252, National Instruments, Austin, TX, U.S.A) to synchronize the motion detection and gait video capture.

In a preliminary experiment, the participant stood at the starting line with his toes just behind the line. The participant was asked to walk through a 6-m corridor decorated with a navy curtain, and the 3-m GAITRite® walkway for steady-state gait was defined by two pairs of infrared sensors that were aligned with the start and finish lines. When the infrared beam was broken by the participant's advancing lower leg, the infrared reflector transmitted a TTL logic signal to the LabVIEW utility on the PC side via a serial RS232 port, providing timestamps to determine the timing of the closest playback frame at the start and end of each walking trial.

The GAITRite® system and the Panasonic video camera (model PV-GS400) simultaneously collected footstep data during the steady-state walking period. The gait sequence image frame and the ^{1st}KPC waveform of a healthy subject are shown in Figure B2 (a) and (b), respectively.

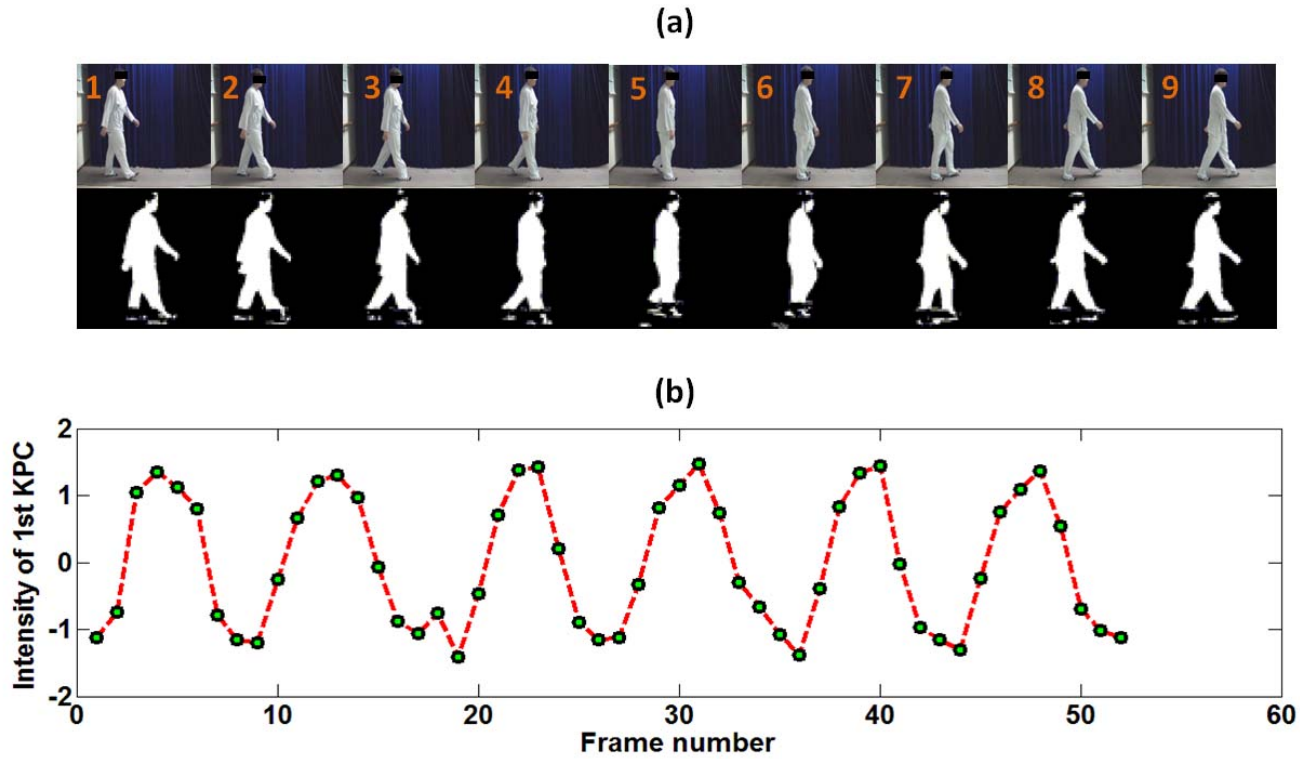

Figure B2. Sequential gait image frames from a healthy subject walking on the GAITRite walkway system. (s) The top panels are original sequential walking image frames containing 240 × 320 pixels. The bottom panels are trimmed 64 × 64 pixel binary silhouettes of the top panels. (b) The ^{1st}KPC waveform of a selected non-PD subject participating in the preliminary experiment. The green dots indicate the magnitudes of the sequential $^{1st}KPCs$.

Results from the KPCA-based method were acquired using processing procedures identical to those used in the actual experiment. A paired Student's *t*-test was conducted to examine the differences between the gait parameters (gait cycle time, stride length, walking velocity and cadence) measured by the GAITRite® system and the KPCA-based method. According to table B.1, there were no significant differences (*p*-value > 0.05) in the gait cycle time, stride length, walking velocity, or cadence detected using these two methods, indicating that the KPCA-based method and the GAITRite® system yielded comparative gait measurements. This finding was expected because the results of the two methods were also correlated with respect to the spatial measures recorded

concurrently during the subject's walking trials. We are hence convinced of the validity of the KPCA-based method for acquiring adult gait cycle time, stride length, walking velocity, and cadence.

Table B1 Comparison of gait parameters assessed by the GAITRite® system and the KPCA-based method

Gait Parameters	KPCA	GAITRite®	*p-value*
Gait cycle time (s)	1.26±0.13	1.26±0.12	N.S.
Stride Length (cm)	116.81±6.55	116.48±6.68	N.S.
Walking Velocity (cm/sec)	92.95±10.55	92.97±10.59	N.S.
Cadence (steps/min)	95.90±9.99	95.79±9.97	N.S.

N.S is non-significant ($p > 0.05$).

Appendix C Comparing the CTA-based gait tracking and analysis system with the Vicon system for validation

To evaluate whether the proposed video-based gait tracking and analysis system in chapter 3 is valid in assisting clinical diagnoses and further applications, the quantification of gait initiation and symmetry from the proposed video-based gait tracking and analysis system is compared with the quantification outcomes from a commercial system, the Vicon system (Vicon Inc, Oxford, UK).

The Vicon system is a commercially available motion analysis technology that uses optical reflective markers to measure three dimensional movement for capturing and modeling human motion [105]. In the experiment comparing the proposed system to the Vicon system, five healthy volunteers (4 males and 1 female) with an average age of 23.8 years (max = 25, min = 23, S.D. = 0.84) are recruited and given informed consent. The Vicon system and proposed video-based system are synchronized for the simultaneous collection of temporal-spatial gait parameters performed by the recruited subjects. Each volunteer was asked to perform four successful trials at their natural pace during the trials to naturally reflect their gait performance. Gait cycle time, stance phase, stride length, walking velocity, and cadence, were calculated to obtain comparison.

A two-sample (paired) *t*-test was conducted to examine the differences. According to table C1, *p*-values greater than 0.05 were obtained for all comparisons of temporal-spatial gait parameters across the two systems. There are no significant differences between the proposed system and the Vicon system; results obtained from the proposed system are comparable to those from the Vicon

system. Thus, the proposed system exhibits validity for acquiring temporal-spatial gait measurements of interest.

Table C1. Comparisons of several gait parameters with VICON System.

Gait Parameters	Our system	VICON	*p*-value
Gait cycle time (sec)	1.39±0.19	1.37±0.19	0.757
Stance Phase (%)	64.83±2.07	63.90±2.92	0.239
Stride Length (cm)	92.32±5.51	92.71±6.10	0.825
Walking Velocity (cm/sec)	67.70±10.35	68.93±10.47	0.706
Cadence (steps/min)	87.82±11.05	89.08±11.57	0.719